UNIVERSITY OF TORINO
DEPARTMENT OF MEDICAL SCIENCES
DOCTORAL PROGRAMME IN MEDICAL PHYSIOPATHOLOGY – XXXVI CYCLE

THESIS

STUDY ON miRNA EXPRESSION IN URINARY EXTRACELLULAR VESICLES OF PATIENTS UNDER MODULATION OF SODIUM INTAKE

CANDIDATE: Dr. Fabrizio BUFFOLO

TUTOR: Prof. Paolo MULATERO

ACADEMIC YEARS: 2020-2023

LIST of CONTENTS

LIST of TABLES & FIGURES

1. INTRODUCTION

Dietary sodium excess is responsible for an estimate of 1.89 million of deaths worldwide in 2019, with a burden that progressively increased over the last three decades[1]. High sodium consumption is associated with increased blood pressure levels[2,3]cardiovascular events[3] and chronic kidney disease[1]. Robust evidence indicates that the reduction of sodium intake reduces blood pressure levels[4] and cardiovascular risk[5]. The global mean sodium intake is 4 g/day (10 g/day of salt) and international guidelines recommend a reduction of sodium consumption to less than 2 g/day (<5 g/day of salt)[6,7]. Considering the poor adherence of the population to low sodium diet (LSD), understanding the mechanisms of sodium-induced hypertension and organ-damage is currently an important unmet medical need.

The hemodynamic changes induced by sodium load, explain only a part of the long-term deleterious effects of high sodium diet (HSD)[8,9]. However, the majority of the studies investigating the pathophysiological mechanisms of sodium excess comes from pre-clinical research in animal models[8,9].

Extracellular vesicles (EVs) are bilayer membrane-bound structures released by all cells types, which carry various cargos, including nucleic acids (such as small non-coding RNAs, messenger [mRNAs] and DNA fragments), proteins, lipids, and metabolites[10]. EVs can be isolated from cell cultures, biofluids [10], and tissues[11] and their cargos reflect the activation state of parental cells. EVs allows cell-to-cell paracrine and endocrine communication, influencing the content and biological processes of the recipient cells[10,12].

In kidney, in presence of an intact glomerular filtration barrier, circulating EVs cannot cross the glomerular membrane pores[13]. Therefore, in normal condition, urinary EVs (uEVs) derives primarily from the cells of the nephron lumen and the urinary tract[13,14]. This feature makes uEVs a non-invasive tool for the characterization of renal biological processes in different disease or pathophysiological conditions.

MicroRNAs (miRNAs) are small non-coding RNA abundantly released into EVs, that complementarily bind the 3′UTR of target mRNAs, regulating mRNA degradation and translation[15]. miRNAs are stable molecules and, when transported within EVs, they are able to target distant sites and regulate gene expression with a hormone-like function[10].

The aim of this prospective study is to investigate the impact of dietary sodium modulation on renal biological processes, through the evaluation of small non-coding RNAs content in 24-hour urinary EVs isolated from high-risk normotensive subjects who underwent tightly controlled sodium-restricted and sodium-loaded diet. After the identification of differentially expressed miRNAs among the two dietary regimen, we identified mRNAtargets and performed a bioinformatic network analysis to identify the pathways uniquely enriched following each specific diet. Hence, we selected specific miRNA-mRNA target pairs, considered as potential drivers of sodium mediated effects at renal levels, and we validated the miRNA-mRNA target regulation using human tubular cells as *in vitro* model.

2. MATERIALS AND METHODS

2.1 *Participant selection*

The protocol was approved by the local ethical committee. Written informed consent was obtained from all the patients recruited in the study. Individuals aged between 35 and 70 were prospectively enrolled. We included subjects with SBP comprised between 120 and 135 mmHg and DBP comprised between 75 and 85 mmHg. Main exclusion criteria were: known history of hypertension or use of antihypertensive medications, previous cardiovascular events or estimated glomerular filtration rate <60 mL/min/1.73m^2. The complete list of inclusion and exclusion criteria is listed below.

Inclusion criteria (high-risk normotensive):

1. Age 35-70 years
2. Systolic blood pressure of 120-135 mmHg and/or diastolic blood pressure of 75-85 mmHg
3. At least one, or more, of the following:
    - BMI ≥ 25 kg/m2
    - Family history of hypertension prior to the age of 60 years in a parent or sibling
    - Diabetes with a hemoglobin A1c < 9%
4. If systolic blood pressure is 115-120 mmHg and/or diastolic blood pressure is 70-75 mmHg, must have two or more of the following:
    - BMI ≥ 25 kg/m2

- Family history of hypertension prior to the age of 60 years in a parent or sibling
- Diabetes with a hemoglobin A1c < 9%

Exclusion criteria:

1. Known history of hypertension or use of antihypertensive medications
2. Known history of stroke, coronary artery disease, myocardial infarction, heart failure, cerebral or aortic aneurysm, or preeclampsia.
3. Active cancer that is being treated with chemotherapeutic agents
4. Pregnancy
5. Breast feeding
6. Daily use of prescribed opioid medications
7. Illicit drug use (cocaine, heroin, methamphetamine)
8. Daily non-steroidal anti-inflammatory medication use
9. Daily use of glucocorticoids
10. Electrocardiogram that shows evidence of prior myocardial infarction, atrial arrhythmia, left or right bundle branch blocks.
11. Estimated glomerular filtration rate < 60 mL/min/1.73m2
12. Active and untreated hyper- or hypo-thyroidism
13. Abnormal screening laboratories (comprehensive of complete blood count, thyrotropin) or endocrinological diseases

All individuals were studied after 5 to 7 days of 2 different dietary conditions: sodium restricted (low sodium diet; LSD) and sodium loaded diet (high sodium diet; HSD) (Figure 1). Sodium restriction was achieved by providing meals with less than 40 mmol of sodium/day, while sodium loading was achieved with more than 180 mmol of sodium/day. Potassium and calcium intake was maintained constant in both diets: 75 mmol of potassium/day, and 600 mg of calcium/day. Compliance to the dietary regimen was assessed by 24h urinary sodium excretion. All subjects underwent 24-hour ambulatory blood pressure with liberal diet. Office systolic blood pressure (SBP) and diastolic blood pressure (DBP), plasma renin activity (PRA) and aldosterone concentration were measured after each specific diet. Plasma aldosterone concentrations was measured by enzyme-linked immunosorbent assay (ELISA) (IBL International [Catalog RE52301]; Hamburg, Germany). The lowest reportable was 0.2 ng/dL and a dynamic range of 0.57-100 ng/dL, inter-assay CV= 8.6-9.4%, intra-assay CV= 5.6-9.7%. PRA was measured by ELISA (IBL-America; Minneapolis, MN; inter-assay CV= 4.8-7.1%, intra-assay CV= 6.3-8.7%). A 24-hour urine collection was obtained after 5 to 7 days of each dietary condition. Sample were aliquoted, stored, and shipped at room temperature in Urine Collection and Preservation Tubes (Norgen, #18111).

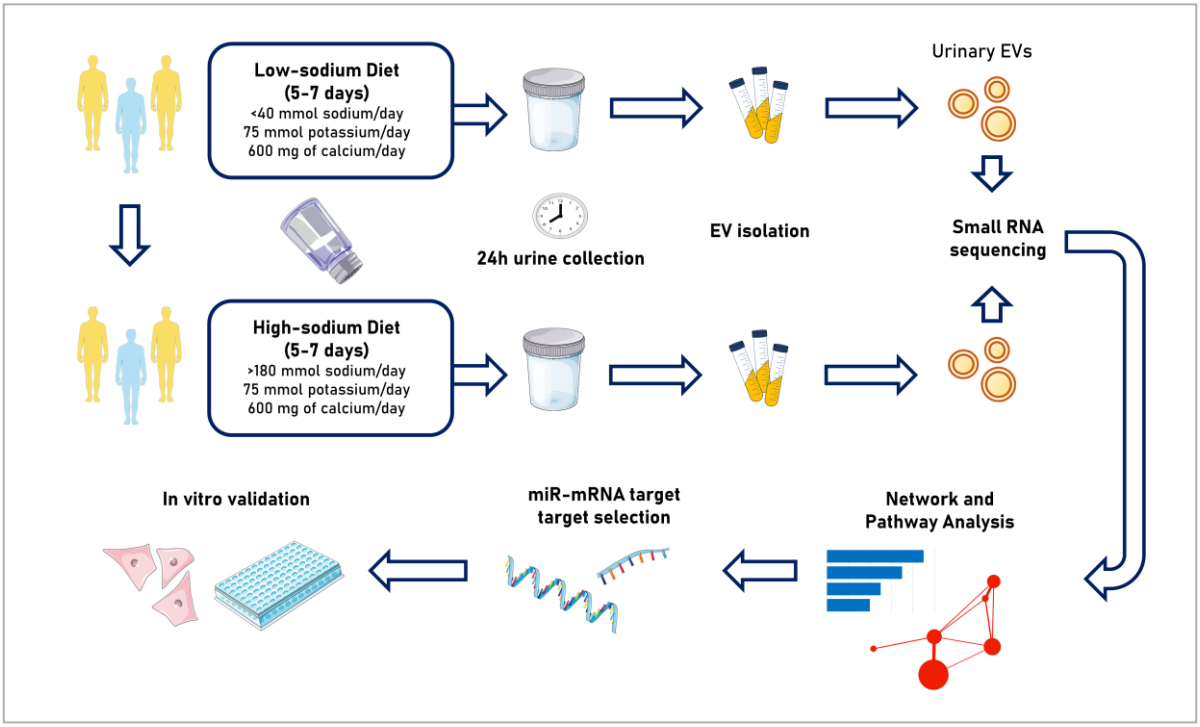

Figure 1. Design of the study. *We prospectively recruited 14 subjects with high risk normotension, that underwent 5-7 days of low sodium diet (<40 mmol/day or 0.92 g/day) or high sodium diet (>180 mmol/day or 4.14 g/day). At the end of each diet, we isolated urinary EVs (uEVs) from 24h urine collection through serial centrifugation and ultracentrifugation. We then performed small-RNA sequencing of uEVs and bioinformatic analysis to select miRNA-mRNA target for in vitro validation. We finally validated miRNA-target regulation in human tubular cell lines (HK-2 cells).*

2.2 *EVs isolation and characterization*

uEV isolation and characterization complied with recommendations of the International Society for Extracellular Vesicles[14]. Twenty mL of urine samples were centrifuged for 10 minutes at 1000g at 4°C to remove cells and debris and then filtered with 0.45 µm filter. The filtered supernatant was centrifuged for 10 minutes at 2500g at 4°C. The supernatant was collected and EVs were pelleted by ultracentrifugation (Optima L-90K ultracentrifuge, Beckman Coulter) at 100,000g for 3 hours at 4°C (Rotor 45 Ti, polycarbonate tubes, Beckman Coulter). Pellets

containing uEVs were suspended in: 1) phosphate-buffered saline (PBS) for nanoparticle tracking analysis (NTA) and transmission electron microscopy; 2) in RIPA buffer (Thermo Fisher Scientific) for Western Blots, and finally 3) in QIAzol Lysis Reagent (Qiagen) for nucleic acids extraction and sequencing.

uEVs were analyzed for diameter and quantified using Nanosight LM10 (NanoSight Ltd. The presence of EV specific markers (CD63 and CD81), cell specific marker (calnexin), and protein contaminant (uromodulin) was assessed by Western Blotting. We assessed EV integrity and morphology by transmission electron microscopy (TEM).

2.3 *Nanoparticle Tracking Analysis (NTA)*

Vesicle diameter and particle abundance were determined by NTA (NanoSight LM10 system, Salisbury, UK). The pellet from ultracentrifugation (UC) was diluted in PBS and injected in the NanoSight. For each sample, 3 videos of 60 s duration were recorded. Camera level was set at 9 for all the acquisitions and screen gain at 1. The size and concentration from the 3 measurements of each sample were normalized to obtain the distribution in each condition. uEV concentration was expressed as number of particles per 1 mL.

2.4 *Western Blot*

Western Blot analysis was performed on protein lysate (RIPA buffer, Thermo Fisher Scientific) after UC for uEVs and after centrifugation for cells. Protein quantification was performed by the bicinchoninic acid assay (BCA, Pierce),

reading at 560 nm against standard curve. Membranes were incubated overnight at 4°C under gentle agitation with primary antibodies diluted in Everyblot Blocking Buffer (BioRad, #12010020). Membranes were incubated with HRP-conjugated goat anti-rabbit and anti-mouse secondary Ab (Pierce, Thermo Fisher Scientific; 1:5000 dilution in Everyblot Blocking Buffer) at RT for 2 h. The signal was detected by using a chemiluminescent substrate SuperSignal West Femto Maximum Sensitivity Substrate (Thermo Fisher Scientific) and visualized with the ChemiDoc™ MP Imaging System (BioRad). Blots of 4 representative samples of uEVs, cell control and urine control were incubated with the following primary antibodies: mouse monoclonal anti-CD63 (Abcam, ab193349, 1:1000), rabbit monoclonal anti-CD81 (Abcam, ab109201, 1:500), rabbit monoclonal anti-UMOD (Abcam, ab207170, 1:1000), and rabbit polyclonal anti-calnexin (Abcam, ab22595, 1:1000). Blots for *in vitro* experiments, with HK-2 cells, were incubated with the following antibodies: rabbit polyclonal anti-PPAR alpha (abcam, ab3484, 1:500) and rabbit monoclonal anti-vinculin (abcam, ab129002, 1:10.000).

2.5 *Transmission Electron Microscopy (TEM)*

Analysis of transmission electron microscopy of representative samples was performed by incubating EV preparations on 200 mesh nickel formvar carbon-coated grids (Electron Microscopy Science, Hatfield, PA, USA) for 20 min. Next, fixation was obtained by incubating grids with 2.5% glutaraldehyde containing 2% sucrose and repeating washing steps were done in distilled water. Finally, samples were negatively stained with Nano-W and NanoVan (Nanoprobes, Yaphank, NY,

USA) and analyzed using a Jeol JEM 1010 electron microscope (Jeol, Tokyo, Japan).

2.6 *RNA isolation*

Once uEVs were resuspended in 700 µl of QIAzol Lysis Reagent, samples were vortexed for 1 min, and total RNA was extracted using the miRNeasy Mini Kit (Qiagen, #217004) according to the manufacturer's protocol. Each sample was eluted twice in 30 µl of RNase-free water.

RNA quality and quantity were verified according to MIQE guidelines[16]. For all samples, RNA concentration was quantified by Invitrogen Qubit® 4 Fluorometer with Qubit® microRNA Assay Kit (Invitrogen, Milan, Italy).

2.7 *Library preparation for small RNA sequencing*

Small RNA transcripts were converted into barcoded cDNA libraries as previously described [17]. Briefly, library preparation was performed with the NEBNext Multiplex Small RNA Library Prep Set for Illumina (Protocol E7330; New England BioLabs Inc., USA). For each library, 6 µL of RNA (min 35 ng) were used in all the experimental procedures as starting material. A unique indexed primer was used for each library so that all the libraries could be pooled into one sequencing lane. Multiplex adaptor ligations, reverse transcription primer hybridization, reverse transcription reaction, and PCR amplification were performed according to the protocol for library preparation. After PCR amplification, the cDNA constructs were purified with the QIAQuick PCR Purification Kit (Qiagen, Germany)

following the modifications suggested by the NEBNext Multiplex Small RNA Library Prep Protocol E7330 and loaded on the Bioanalyzer 2100 (Agilent Technologies, Italy) using the DNA High Sensitivity Kit (Agilent, Germany) according to the manufacturer's protocol. Libraries were pooled together (36-plex) and further purified with a gel size selection.

A final Bioanalyzer 2100 run with the High Sensitivity DNA Kit (Agilent Technologies, Milan, Italy) allowed the final analysis of DNA libraries regarding size, purity and concentration. The obtained libraries were subjected to the Illumina sequencing pipeline, passing through clonal cluster generation on a single-read flow cell and 75 cycles sequencing-by-synthesis on the NextSeq500 sequencer (Illumina Inc.).

2.8 *Computational and Statistical Analyses*

Raw reads adapter clipping was performed with the Cutadapt software (version 1.18) [18]. Reads longer than 14 nucleotides were mapped to a sncRNA reference with the bwa alignment software (version 0.7.17-r1188) [19], using the mem algorithm and a seed length of 10. Only alignments without mismatches or indels were considered and those with the highest quality were used to assign each read to a unique sncRNA. Thus, sncRNAs were quantified for each sample and then merged into a single count matrix, setting missing sncRNAs to zero. Differential expression analysis was performed with the DESeq2 Bioconductor's package (version 1.22.2) [20]. For each model, samples with missing covariates were dropped and only sncRNAs, where at least 70% of the remaining samples had counts greater

than 5, were tested. sncRNAs were considered significantly associated with a condition or a trend if their p-value, after adjustment for multiple testing by FDR, was below the 0.05 threshold.

2.9 *Pathway and network analyses*

Validated miRNA target genes of differentially expressed miRNAs were obtained by MiRTarBase (retrieved in July 2023) and used for the following analysis [21]. Enriched "Reactome 2022" pathways were generated by testing MiRTarBase-derived gene targets with EnrichR [22]. We performed adjustment of p-value with Benjamini-Hochberg to calculate q-values, for controlling for multiple comparisons. Pathways uniquely enriched in each condition (high- *versus* low-sodium diet) were considered for pathway and network analysis. Considering the canonical inhibitory effect of miRNAs on validated mRNA targets, we attributed the enriched pathways to high- *versus* low-sodium diet on the basis of predicted "up-regulated" gene targets. The -log(q value) was calculated for pathway bar graph and network analysis.

The pathway network and cluster analysis were designed with Gephi 0.9.2. The nodes represent enriched pathways and the node size is proportional to -log(q-value) of each pathway. For clarity of representation, pathways with -log(q-value)< 1.5 were excluded in "low sodium diet" network and -log(q-value)< 2.0 in "high sodium diet". Connection thickness is proportional to the Jaccard Index, which estimates pathway similarity between nodes. For clarity of representation, pathways with Jaccard Index< 0.1 were excluded in "low sodium diet" network and Jaccard

Index< 0.3 in “high sodium diet”. Unbiased clustering of pathways was obtained through modularity assessment [23].

miRNA-mRNA target analysis was performed using differentially down-regulated miRNAs for each condition and respective mRNA targets (that are therefore up-regulated). mRNA targets from specific clusters of interest were highlighted in green. In miRNA-mRNA target analysis of “high sodium diet”, the connection between miR-320b and *ICAM-1*, although not present in MiRTarBase, was added manually since validated by the previously published study of Gidlöf et al. [24].

2.10 *In vitro experiments*

Human kidney 2 (HK-2) cells were cultured in Dulbecco's Modified Eagle Medium (DMEM) (Thermo Fisher Scientific, # 11885084) supplemented with 10% fetal bovine serum (Thermo Fisher Scientific, #11885084). HK-2 cells were transfected with Lipofectamine 2000 Reagent (Invitrogen, #11668027) according to manufacturer’s instructions. miRvana miRNA inhibitors for hsa-miR-320b and hsa-miR-10b-5p (Applied Biosystems, #4464084) were transfected at a concentration of 30 nM for each miRNA inhibitors. Controls were transfected with Lipofectamine 2000 Reagent alone. Lysate for miRNA and mRNA isolation was obtained 24 hours after transfection, while material for protein detection and quantification was obtained after 48 hours.

2.11 *RNA and miRNA analysis*

RNA was extracted using the miRNeasy Mini Kit (Qiagen, #217004). Reverse transcription of miRNAs was performed with Taqman Advanced miRNA cDNA Synthesis Kit (Applied Biosystems, #A28007) and miRNAs were detected and quantified through quantitative real-time polymerase chain reaction (qRT-PCR) with the following TaqMan Advanced miRNA Assay (Applied Biosystems, #A25576): 478588_mir (hsa-miR-320b), 478494_mir (hsa-miR-10b-5p) and 477860_mir (hsa-miR-16-5p). Expression levels were normalized to the miR-16-5p, used as endogenous control. For mRNA, cDNA was made using iTaq universal probe supermix (BioRad, # 1725132). qRT-PCR was performed using the following Taqman Gene Expression Assays (Applied Biosystems, #4453320): Hs02786624-g1 (*GAPDH*), Hs00164932_m1 (*ICAM-1*), Hs00947536_m1 (*PPAR-α*). RNA quantification was performed using ABI 7500 Fast Real-Time PCR System (Applied Biosystems). Samples were run in duplicate and gene expression levels were analyzed with the $2^{-\Delta\Delta CT}$ relative quantification method. Expression levels were normalized to glyceraldehyde 3-phosphate dehydrogenase (*GAPDH*), adopted as endogenous control.

2.12 *Flow Cytometry*

Cells were detached from the well plate using Cell Dissociation Solution Non-enzymatic 1x (Sigma-Aldrich, #C5914) with 30 min of incubation, centrifuged at 2.000 g for 5 min and resuspended in 100 µL of PBS. The pellet was then incubated with CD54 (ICAM-1) Monoclonal Antibody (HA58), PE (eBioscience, #12-0549-41) and incubated for 30 min on ice, covered by light. The samples were washed in

PBS and centrifuged at 2.000 g for 5 min and suspended in 100 µL of PBS. CytoFLEX Flow Cytometer (Beckman Coulter) was used

for data acquisition.

2.13 *Statistical analysis*

IBM SPSS Statistics 28 (IBM, New York), GraphPad PRISM 9.0 (La Jolla, CA) were used for statistical analysis. Variables were treated as parametric or non-parametric according to their distribution. Normally distributed variables were reported as mean ± standard deviation and analyzed by Student t test for independent samples and paired t test for dependent samples. Non-normally distributed variables were expressed as median (interquartile range) and analyzed by Mann-Whitney U test was applied for independent variables and Wilcoxon signed-rank test for paired variables. Categorical variables were expressed as absolute number and percentage, and analyzed by a $\chi 2$.

3. RESULTS

3.1 *Subject characteristics*

A total of 14 subjects were recruited with a mean age of 59±8 years, BMI of 31.0±4.4 kg/m^2 and 24h ambulatory blood pressure values within the normal range (Table 1). All the subjects underwent 5-7 days of LSD and HSD. 24h urinary sodium excretion showed high adherence to the prescribed diet [average 183.0 (108.7-255.6) mmol/d in HSD versus 14.6 (7.7-24.2) mmol/d in LSD]. Aldosterone and PRA were significantly reduced after HSD, reflecting the expected suppression of renin-angiotensin-aldosterone system following sodium load.

Table 1

	Subjects (n=14)		
Age (years)	59±8		
Gender (%) **Female** **Male**	 6 (42.9) 8 (57.1)		
BMI (kg/m^2)	31.0±4.4		
ABPM 24h SBP (mmHg)	116±10		
ABPM 24h DBP (mmHg)	69±9		
	LSD	**HSD**	***p*-value**
SBP (mmHg)	119±10	115±9	0.291
DBP (mmHg)	78±6	70±9	<0.001
PRA seated (ng/ml/h)	3.25 (1.88-6.15)	0.40 (0.10-0.85)	0.001
Aldosterone seated (ng/dl)	22.1 (17.7-28.0)	7.9 (5.4-12.3)	<0.001
24h urinary volume (ml)	1675 (1300-2343)	1845 (1500-2502)	0.109
Urinary sodium spot (mmol/l)	11.7 (5.3-12.7)	93.5 (61.8-109.6)	<0.001
24h urinary sodium (mmol/d)	14.6 (7.7-24.2)	183.0 (108.7-255.6)	<0.001

Table 1. Clinical and biochemical characteristics of enrolled subjects. *The table shows the clinical characteristics of recruited subjects and biochemical features after low sodium diet (LSD) and high sodium diet (HSD). Variables are reported as mean±standard deviation, median (interquartile range), or absolute number (percentage, %), as appropriated. ABPM, ambulatory blood pressure measurement; BMI, body mass index; DBP, diastolic blood pressure; PRA, plasma renin activity; SBP, systolic blood pressure. Differences were considered significant when P<0.05.*

3.2 *uEVs characterization and small-RNA sequencing*

To investigate the enrichment of small-RNA cargos in uEVs after LSD and HSD, we isolated uEVs from 24h urine collection, through serial centrifugation and 3h ultracentrifugation (Figure 1). We characterized uEV size, distribution, morphology and protein content through NTA, Western Blot and TEM as showed in (Figure 2).

Small-RNA sequencing identified 111 small-RNAs (Figure 3C), including 30 differentially expressed between the 2 diets (Figure 3A-Table 2): 21 piwi-interacting RNAs (piRNAs), 8 miRNAs and 1 ribosomal (rRNA) (Figure 3D). Focusing on miRNA expression, 63 miRNAs were identified in uEVs, including 8 miRNAs differentially expressed in the 2 dietary conditions (Figure 3B). miR-320a-3p, miR-99a-5p, miR-320b and miR-221-3p resulted significantly up-regulated under LSD (Figure 3E); let-7f-5p, miR-10a-5p, miR-10b-5p and miR-27b-3p were significantly up-regulated under HSD (Figure 3F).

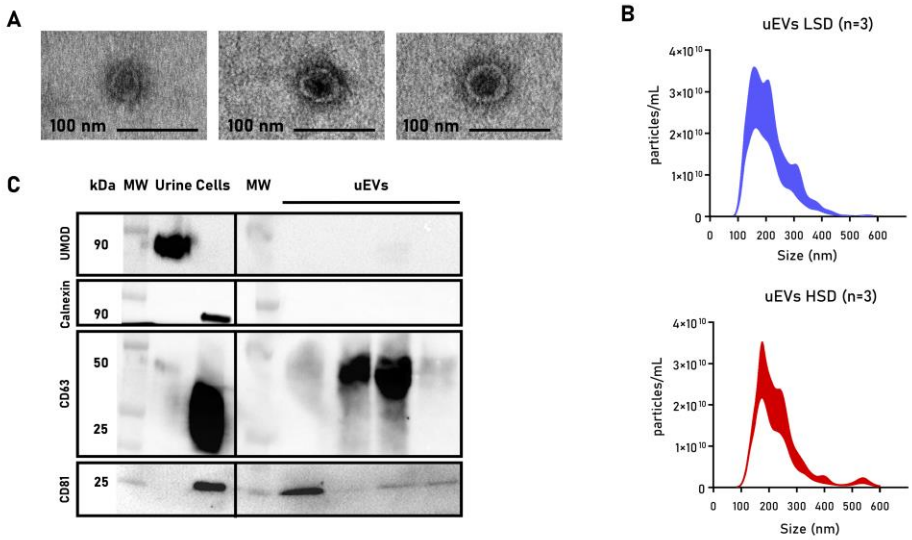

Figure 2. Characterization of urinary extracellular vesicles (uEVs). *(A) Transmission electron microscopy: representative images of EVs purified from urine by ultracentrifugation. (B) Cumulative distribution plot combining nanoparticle concentration (number of particles per mL; y axis) and diameter (nm; x axis) in high-sodium diet (HSD) and low-sodium diet (LSD). (C) Western Blot analysis of uromodulin (90 kDa), calnexin (90 kDa), CD63 (25–55 kDa), and CD81 (25 kDa). Representative blots are shown for total urine, human proximal tubular cells, and uEVs collected after ultracentrifugation from 4 urine samples.*

Table 2

Gene_name	log2(FoldChange)	lfcSE	-log(q-value)
piRNA:piR-hsa-25783	-1.86	0.19	19.23
piRNA:piR-hsa-28489	-3.75	0.52	10.41
piRNA:piR-hsa-32159	-1.00	0.14	9.76
piRNA:piR-hsa-25782	-1.77	0.28	7.87
piRNA:piR-hsa-23248	-1.87	0.35	5.58
piRNA:piR-hsa-9010	-2.24	0.43	5.52
piRNA:piR-hsa-23317	-1.53	0.30	5.12
rRNA:RNA5SP162-ENST00000516014.2	-1.72	0.37	4.40
piRNA:piR-hsa-1191	-2.13	0.50	3.54
piRNA:piR-hsa-12719	-1.96	0.48	3.35
piRNA:piR-hsa-182	-1.87	0.46	3.25
piRNA:piR-hsa-23533	-1.42	0.38	2.77
piRNA:piR-hsa-1177	-1.38	0.37	2.75
piRNA:piR-hsa-2106	0.91	0.28	2.09
piRNA:piR-hsa-28488	-1.48	0.47	1.97

Gene_name	log2(FoldChange)	lfcSE	-log(q-value)
miRNA:hsa-miR-320a-3p	-0.84	0.27	1.97
piRNA:piR-hsa-23574	-1.31	0.43	1.79
piRNA:piR-hsa-7201	-1.23	0.41	1.76
piRNA:piR-hsa-23566	-1.14	0.40	1.67
piRNA:piR-hsa-12790	0.76	0.27	1.67
miRNA:hsa-miR-99a-5p	-0.55	0.19	1.67
miRNA:hsa-miR-320b	-0.92	0.32	1.67
miRNA:hsa-miR-221-3p	-0.63	0.23	1.61
miRNA:hsa-let-7f-5p	0.70	0.25	1.61
miRNA:hsa-miR-10a-5p	0.51	0.19	1.59
miRNA:hsa-miR-10b-5p	0.48	0.17	1.59
miRNA:hsa-miR-27b-3p	0.45	0.17	1.41
piRNA:piR-hsa-28131	-0.56	0.22	1.38
piRNA:piR-hsa-7239	-1.10	0.44	1.35
piRNA:piR-hsa-1207	-0.52	0.21	1.35
miRNA:hsa-miR-423-5p	-0.74	0.30	1.29
piRNA:piR-hsa-28877	-0.62	0.27	1.17
miRNA:hsa-miR-203a-3p	0.47	0.20	1.16
miRNA:hsa-miR-182-5p	0.48	0.21	1.10
miRNA:hsa-miR-22-3p	-0.71	0.33	1.04
miRNA:hsa-miR-191-5p	-0.44	0.21	1.01
piRNA:piR-hsa-11361	0.75	0.37	0.91
piRNA:piR-hsa-28223	-0.66	0.33	0.91
miRNA:hsa-miR-101-3p	0.73	0.36	0.91
miRNA:hsa-miR-27a-3p	0.45	0.22	0.91
miRNA:hsa-miR-378a-3p	-0.52	0.26	0.91
miRNA:hsa-miR-30e-3p	0.43	0.22	0.90
miRNA:hsa-miR-148a-3p	0.49	0.25	0.89
piRNA:piR-hsa-5067	-1.04	0.54	0.87
piRNA:piR-hsa-27493	-0.48	0.25	0.86
miRNA:hsa-miR-200b-3p	0.30	0.16	0.86
miRNA:hsa-miR-30c-5p	0.34	0.18	0.82
piRNA:piR-hsa-5938	0.73	0.40	0.79
piRNA:piR-hsa-24672	0.69	0.40	0.75
miRNA:hsa-miR-30a-3p	0.28	0.16	0.75
piRNA:piR-hsa-5937	0.70	0.40	0.75
miRNA:hsa-let-7i-5p	-0.24	0.14	0.70
miRNA:hsa-let-7a-5p	0.50	0.31	0.67
miRNA:hsa-miR-9-5p	0.44	0.28	0.63
piRNA:piR-hsa-9491	0.81	0.51	0.63
piRNA:piR-hsa-619	-0.63	0.43	0.55
miRNA:hsa-miR-26a-5p	0.25	0.17	0.54

Gene_name	log2(FoldChange)	lfcSE	-log(q-value)
miRNA:hsa-miR-181a-5p	-0.38	0.27	0.51
miRNA:hsa-miR-423-3p	-0.32	0.24	0.47
miRNA:hsa-miR-128-3p	0.33	0.25	0.47
miRNA:hsa-miR-429	0.32	0.26	0.41
miRNA:hsa-miR-28-3p	-0.24	0.20	0.39
miRNA:hsa-miR-24-3p	-0.23	0.19	0.37
miRNA:hsa-miR-363-3p	-0.36	0.31	0.37
piRNA:piR-hsa-28875	0.43	0.37	0.36
miRNA:hsa-miR-200c-3p	0.23	0.20	0.36
miRNA:hsa-miR-30b-5p	-0.43	0.39	0.35
miRNA:hsa-let-7e-5p	0.31	0.30	0.32
miRNA:hsa-miR-532-5p	0.14	0.14	0.32
miRNA:hsa-miR-26b-5p	0.26	0.27	0.26
miRNA:hsa-let-7g-5p	0.20	0.22	0.26
piRNA:piR-hsa-7193	-0.22	0.26	0.22
piRNA:piR-hsa-2107	0.20	0.23	0.22
piRNA:piR-hsa-27616	-0.32	0.38	0.21
miRNA:hsa-miR-29a-3p	-0.23	0.29	0.20
miRNA:hsa-miR-92a-3p	0.19	0.25	0.19
miRNA:hsa-let-7c-5p	0.22	0.30	0.19
miRNA:hsa-miR-186-5p	-0.23	0.31	0.19
piRNA:piR-hsa-27621	-0.24	0.33	0.18
miRNA:hsa-miR-23b-3p	-0.20	0.28	0.18
Mt_tRNA:MT-TS2-ENST00000387449.1	-0.29	0.41	0.18
miRNA:hsa-miR-100-5p	-0.14	0.20	0.18
miRNA:hsa-miR-146b-5p	0.14	0.22	0.16
miRNA:hsa-miR-146a-5p	-0.21	0.33	0.16
Mt_tRNA:MT-TE-ENST00000387459.1	-0.23	0.37	0.15
miRNA:hsa-miR-99b-5p	-0.12	0.20	0.15
miRNA:hsa-let-7b-5p	0.13	0.23	0.12
miRNA:hsa-miR-151a-3p	-0.09	0.17	0.12
miRNA:hsa-miR-30a-5p	0.11	0.23	0.11
miRNA:hsa-miR-222-3p	-0.12	0.25	0.11
piRNA:piR-hsa-20266	0.11	0.24	0.10
miRNA:hsa-miR-21-5p	0.10	0.24	0.10
piRNA:piR-hsa-23231	0.16	0.35	0.10
piRNA:piR-hsa-27282	-0.21	0.48	0.10
miRNA:hsa-miR-125b-5p	-0.08	0.19	0.10
piRNA:piR-hsa-28212	-0.16	0.49	0.07
piRNA:piR-hsa-24684	0.09	0.28	0.07
miRNA:hsa-miR-194-5p	-0.07	0.22	0.07
miRNA:hsa-miR-30d-5p	0.03	0.11	0.06

Gene_name	log2(FoldChange)	lfcSE	-log(q-value)
miRNA:hsa-miR-103a-3p	0.06	0.26	0.06
piRNA:piR-hsa-27622	0.08	0.37	0.06
miRNA:hsa-miR-125a-5p	0.08	0.31	0.06
miRNA:hsa-miR-192-5p	-0.06	0.25	0.06
miRNA:hsa-miR-200a-3p	0.06	0.25	0.06
Mt_tRNA:MT-TV-ENST00000387342.1	0.09	0.41	0.06
miRNA:hsa-miR-30e-5p	-0.03	0.25	0.02
miRNA:hsa-miR-1246	-0.05	0.77	0.01
piRNA:piR-hsa-28190	-0.01	0.24	0.01
miRNA:hsa-let-7d-5p	-0.01	0.23	0.01
miRNA:hsa-miR-204-5p	0.00	0.16	0.00
piRNA:piR-hsa-24683	0.00	0.25	0.00

Table 2. *Volcano plot of small-RNA in high-sodium diet versus low-sodium diet*

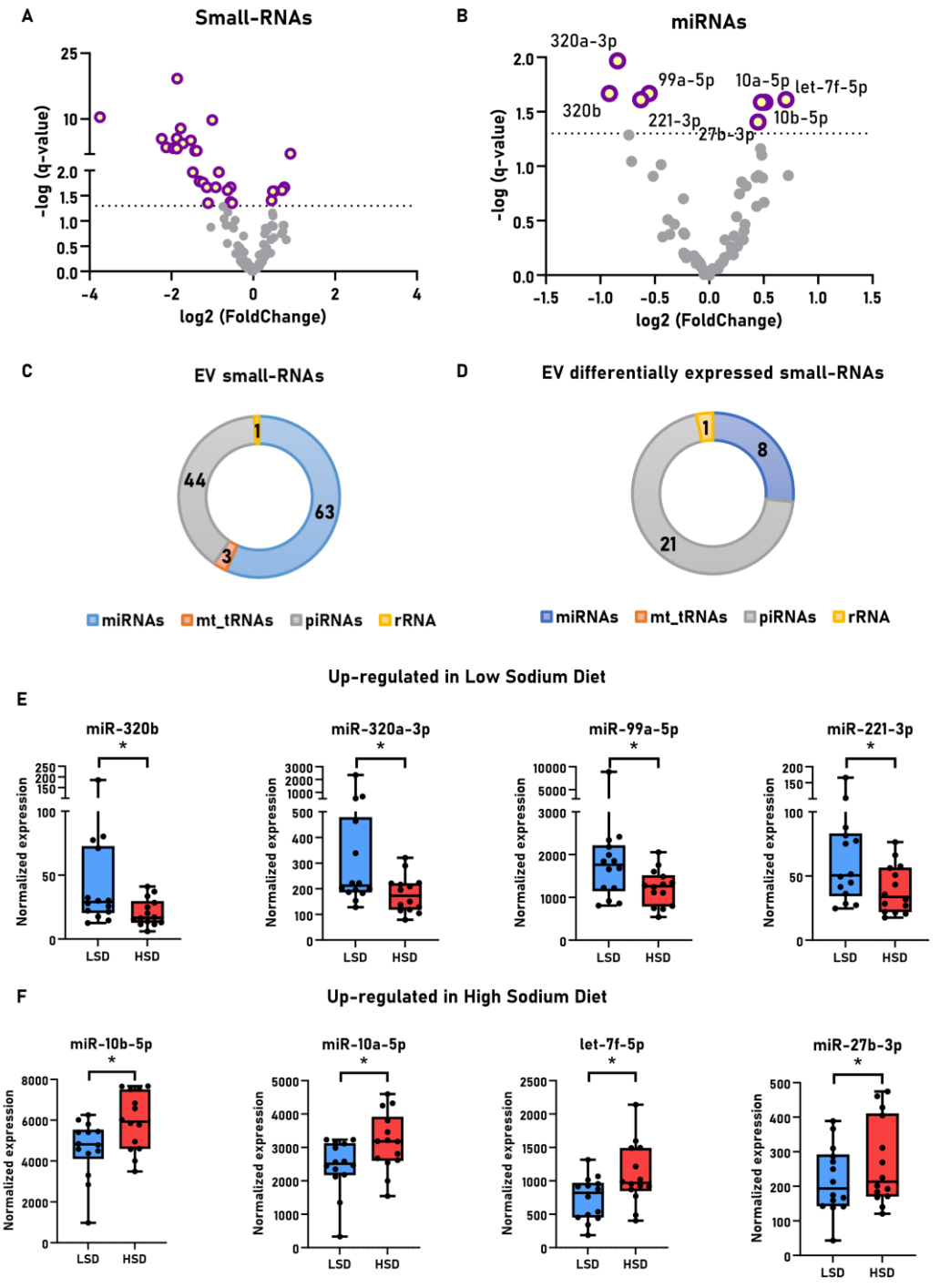

Figure 3. Small-RNA sequencing profiles in urinary extracellular vesicles of 14 subjects after high- and LSD.

(A-B) Volcano plots of all small-RNAs (A) and microRNAs (miRNAs) alone (B) expression levels when compared high and low sodium diet. The dashed line is set at q-value=0.05. Significantly differentially enriched small-RNAs or miRNAs are highlighted in yellow (with violet border). The Y-axis is expressed as -log(q-value);

the x-axis is expressed as log_2 (fold change). (C-D) The ring chart show the proportion of total small-RNAs (C) and differentially expressed small-RNAs (D). (E-F) Dot and box plots of significantly differentially expressed miRNAs up-regulated in low sodium diet (E) and high sodium diet (F).

3.3 *Pathway-network analysis*

To determine the biological role of differentially expressed miRNAs, we used MiRTarBase to predict validated mRNA targets and we considered the canonical function in miRNAs of negative translational regulators of mRNAs. Therefore, for miRNAs down-regulated we expect a following up-regulation of the relative targets. miRNAs down-regulated in HSD targeted 1249 mRNA targets, while miRNAs down-regulated in LSD targeted 1635 mRNA targets. To identify biological processes enriched in each specific dietary condition, we used "Reactome 2022" database for pathway enrichment analysis. For clarity of representation, we showed, for each dietary conditions, the pathways associated with down-regulated miRNAs, thereby associated with predicted up-regulated mRNA targets (Figure 4A-4B; Table 3-4). In HSD, we observed an enrichment of 326 pathways [-log(q-value)>1.5] (Table 3), including those related to translation regulation, immune system, and senescence (Figure 4A). In LSD, we identified an enrichment of 39 pathways [-log(q-value)>1.5] (Table 4), including some related to p53-regulation of cell cycle, white adipocyte differentiation and erythropoietin, platelet-derived growth factor (PDGF) and epidermal growth factor receptor (EGFR) signaling (Figure 4B).

To further investigate the biological effects of differentially enriched mRNA targets, we analyzed the interactions between significantly enriched pathways,

through networks-cluster analysis. In HSD, we identified an enrichment of pathway-clusters related with cell cycle, translation regulation, transforming growth factor beta (TGFβ) pathways and several clusters related to immune system (adaptive and innate immune system, interleukin signaling and interferon signaling) (Figure 4C). In LSD, we identified clusters of pathways related to signaling of erythropoietin and PDGF, p53 transcriptional regulation and peroxisome proliferator-activated receptor (PPAR) transcription pathways (Figure 4D).

Table 3

Term	-log(q-value)	Odds Ratio
Cap-dependent Translation Initiation R-HSA-72737	10.84	6.53
Oncogene Induced Senescence R-HSA-2559585	10.57	18.84
L13a-mediated Translational Silencing Of Ceruloplasmin Expression R-HSA-156827	10.21	6.56
GTP Hydrolysis And Joining Of 60S Ribosomal Subunit R-HSA-72706	10.15	6.48
Formation Of A Pool Of Free 40S Subunits R-HSA-72689	9.83	6.79
Peptide Chain Elongation R-HSA-156902	9.67	7.30
Influenza Infection R-HSA-168255	9.59	4.95
Apoptosis R-HSA-109581	9.33	4.55
Eukaryotic Translation Elongation R-HSA-156842	9.27	6.85
Signaling By ROBO Receptors R-HSA-376176	9.15	4.12
Regulation Of Expression Of SLITs And ROBOs R-HSA-9010553	8.92	4.58
Nonsense Mediated Decay (NMD) Enhanced By Exon Junction Complex (EJC) R-HSA-975957	8.63	5.66
Nervous System Development R-HSA-9675108	8.59	2.64
Eukaryotic Translation Termination R-HSA-72764	8.57	6.47
Response Of EIF2AK4 (GCN2) To Amino Acid Deficiency R-HSA-9633012	8.53	6.10
Nonsense Mediated Decay (NMD) Independent Of Exon Junction Complex (EJC) R-HSA-975956	8.39	6.28
Axon Guidance R-HSA-422475	8.32	2.65
Programmed Cell Death R-HSA-5357801	8.17	3.88
Cellular Response To Starvation R-HSA-9711097	8.15	4.54
Influenza Viral RNA Transcription And Replication R-HSA-168273	8.05	4.79
Selenocysteine Synthesis R-HSA-2408557	7.92	6.10
Viral mRNA Translation R-HSA-192823	7.92	6.10

Term	-log(q-value)	Odds Ratio
Intracellular Signaling By Second Messengers R-HSA-9006925	7.43	3.10
PTEN Regulation R-HSA-6807070	7.32	4.50
PIP3 Activates AKT Signaling R-HSA-1257604	7.23	3.24
SARS-CoV Infections R-HSA-9679506	7.15	2.82
Translation R-HSA-72766	7.14	3.15
SRP-dependent Cotranslational Protein Targeting To Membrane R-HSA-1799339	7.08	5.08
Selenoamino Acid Metabolism R-HSA-2408522	6.63	4.74
Major Pathway Of rRNA Processing In Nucleolus And Cytosol R-HSA-6791226	6.62	3.74
MyD88-independent TLR4 Cascade R-HSA-166166	6.53	4.86
SARS-CoV-2-host Interactions R-HSA-9705683	6.25	3.48
SARS-CoV-2 Infection R-HSA-9694516	6.16	2.95
rRNA Processing R-HSA-72312	6.11	3.42
rRNA Processing In Nucleus And Cytosol R-HSA-8868773	6.11	3.50
MAPK6/MAPK4 Signaling R-HSA-5687128	5.88	5.07
Regulation Of RUNX1 Expression And Activity R-HSA-8934593	5.82	19.81
TRAF6 Mediated Induction Of NFkB And MAP Kinases Upon TLR7/8 Or 9 Activation R-HSA-975138	5.69	4.66
MyD88 Dependent Cascade Initiated On Endosome R-HSA-975155	5.63	4.60
Cyclin D Associated Events In G1 R-HSA-69231	5.61	7.49
Toll Like Receptor 3 (TLR3) Cascade R-HSA-168164	5.58	4.54
Toll Like Receptor 7/8 (TLR7/8) Cascade R-HSA-168181	5.58	4.54
Toll Like Receptor 9 (TLR9) Cascade R-HSA-168138	5.37	4.38
Ribosomal Scanning And Start Codon Recognition R-HSA-72702	5.32	6.31
Translation Initiation Complex Formation R-HSA-72649	5.32	6.31
TP53 Regulates Metabolic Genes R-HSA-5628897	5.31	5.06

Term	-log(q-value)	Odds Ratio
Formation Of Ternary Complex, And Subsequently, 43S Complex R-HSA-72695	5.30	6.87
Cellular Response To Heat Stress R-HSA-3371556	5.26	4.49
Cyclin E Associated Events During G1/S Transition R-HSA-69202	5.24	4.98
mRNA Activation Upon Binding Of Cap-Binding Complex And eIFs, Subsequent Binding To 43S R-HSA-72662	5.24	6.16
FLT3 Signaling R-HSA-9607240	5.23	8.47
Cyclin A:Cdk2-associated Events At S Phase Entry R-HSA-69656	5.10	4.83
Deubiquitination R-HSA-5688426	5.10	2.73
Oxidative Stress Induced Senescence R-HSA-2559580	5.08	4.55
Toll Like Receptor 4 (TLR4) Cascade R-HSA-166016	5.07	3.67
MyD88:MAL(TIRAP) Cascade Initiated On Plasma Membrane R-HSA-166058	5.03	4.09
Transcriptional Regulation By RUNX3 R-HSA-8878159	4.96	4.43
MyD88 Cascade Initiated On Plasma Membrane R-HSA-975871	4.89	4.37
Regulation Of mRNA Stability By Proteins That Bind AU-rich Elements R-HSA-450531	4.83	4.55
G1/S Transition R-HSA-69206	4.61	3.65
Regulation Of NF-kappa B Signaling R-HSA-9758274	4.52	14.07
TAK1-dependent IKK And NF-kappa-B Activation R-HSA-445989	4.30	6.41
SARS-CoV-2 Modulates Host Translation Machinery R-HSA-9754678	4.10	6.04
Transcriptional Regulation By RUNX2 R-HSA-8878166	4.07	3.58
Regulation Of HSF1-mediated Heat Shock Response R-HSA-3371453	4.06	4.35
Host Interactions Of HIV Factors R-HSA-162909	4.02	3.41
Toll-like Receptor Cascades R-HSA-168898	4.00	3.08
Mitotic G2-G2/M Phases R-HSA-453274	4.00	2.92
Insulin-like Growth Factor-2 mRNA Binding Proteins (IGF2BPs/IMPs/VICKZs) Bind RNA R-HSA-428359	3.91	43.87

Term	-log(q-value)	Odds Ratio
Post-transcriptional Silencing By Small RNAs R-HSA-426496	3.91	43.87
Regulation Of PTEN mRNA Translation R-HSA-8943723	3.91	21.07
Deactivation Of Beta-Catenin Transactivating Complex R-HSA-3769402	3.86	6.25
Interleukin-1 Signaling R-HSA-9020702	3.83	3.54
Aberrant Regulation Of Mitotic G1/S Transition In Cancer Due To RB1 Defects R-HSA-9659787	3.68	12.30
Activation Of IRF3/IRF7 Mediated By TBK1/IKK Epsilon R-HSA-936964	3.68	12.30
G2/M Transition R-HSA-69275	3.65	2.82
Metabolism Of Amino Acids And Derivatives R-HSA-71291	3.65	2.20
Class I MHC Mediated Antigen Processing And Presentation R-HSA-983169	3.62	2.17
S Phase R-HSA-69242	3.61	2.95
M Phase R-HSA-68886	3.58	2.16
Interleukin-1 Family Signaling R-HSA-446652	3.54	3.00
MAPK Family Signaling Cascades R-HSA-5683057	3.54	2.27
Defective Intrinsic Pathway For Apoptosis R-HSA-9734009	3.54	8.79
Estrogen-dependent Nuclear Events Downstream Of ESR-membrane Signaling R-HSA-9634638	3.54	8.79
AUF1 (hnRNP D0) Binds And Destabilizes mRNA R-HSA-450408	3.54	5.04
Senescence-Associated Secretory Phenotype (SASP) R-HSA-2559582	3.53	4.01
TCF Dependent Signaling In Response To WNT R-HSA-201681	3.52	2.68
Downregulation Of SMAD2/3:SMAD4 Transcriptional Activity R-HSA-2173795	3.52	7.20
Degradation Of DVL R-HSA-4641258	3.47	4.92
Downregulation Of ERBB2:ERBB3 Signaling R-HSA-1358803	3.47	15.05
Ovarian Tumor Domain Proteases R-HSA-5689896	3.46	6.07
Transcriptional Regulation By VENTX R-HSA-8853884	3.46	6.07
PKMTs Methylate Histone Lysines R-HSA-3214841	3.46	5.38

Term	-log(q-value)	Odds Ratio
Ub-specific Processing Proteases R-HSA-5689880	3.44	2.63
Antiviral Mechanism By IFN-stimulated Genes R-HSA-1169410	3.43	3.89
Stabilization Of P53 R-HSA-69541	3.42	4.81
p53-Dependent G1 DNA Damage Response R-HSA-69563	3.40	4.41
Regulation Of TP53 Activity Thru Methylation R-HSA-6804760	3.40	10.25
Degradation Of Beta-Catenin By Destruction Complex R-HSA-195253	3.38	3.84
ISG15 Antiviral Mechanism R-HSA-1169408	3.35	4.05
mRNA Splicing - Minor Pathway R-HSA-72165	3.31	5.10
HIV Infection R-HSA-162906	3.31	2.47
MTOR Signaling R-HSA-165159	3.30	5.68
G1/S DNA Damage Checkpoints R-HSA-69615	3.28	4.24
Regulation Of PTEN Stability And Activity R-HSA-8948751	3.28	4.24
Autophagy R-HSA-9612973	3.24	3.08
SCF(Skp2)-mediated Degradation Of P27/P21 R-HSA-187577	3.22	4.50
PCP/CE Pathway R-HSA-4086400	3.17	3.63
Signaling By B Cell Receptor (BCR) R-HSA-983705	3.14	3.26
Downstream Signaling Events Of B Cell Receptor (BCR) R-HSA-1168372	3.13	3.80
Mitophagy R-HSA-5205647	3.10	7.03
KEAP1-NFE2L2 Pathway R-HSA-9755511	3.08	3.36
Competing Endogenous RNAs (ceRNAs) Regulate PTEN Translation R-HSA-8948700	3.07	17.54
Chromatin Modifying Enzymes R-HSA-3247509	3.06	2.36
Negative Regulation Of NOTCH4 Signaling R-HSA-9604323	3.03	4.61
MAP Kinase Activation R-HSA-450294	3.03	4.23
PINK1-PRKN Mediated Mitophagy R-HSA-5205685	3.01	8.20

Term	-log(q-value)	Odds Ratio
Response Of Mtb To Phagocytosis R-HSA-9637690	3.01	8.20
Adaptive Immune System R-HSA-1280218	3.01	1.71
Spry Regulation Of FGF Signaling R-HSA-1295596	2.98	10.53
TGF-beta Receptor Signaling In EMT (Epithelial To Mesenchymal Transition) R-HSA-2173791	2.98	10.53
VLDLR Internalisation And Degradation R-HSA-8866427	2.98	10.53
Degradation Of AXIN R-HSA-4641257	2.98	4.50
Regulation Of RUNX3 Expression And Activity R-HSA-8941858	2.98	4.50
Macroautophagy R-HSA-1632852	2.95	3.09
Antigen Processing: Ubiquitination And Proteasome Degradation R-HSA-983168	2.93	2.14
Signaling By CSF3 (G-CSF) R-HSA-9674555	2.92	6.39
G2/M Checkpoints R-HSA-69481	2.92	2.76
Downstream TCR Signaling R-HSA-202424	2.90	3.35
PI3K/AKT Signaling In Cancer R-HSA-2219528	2.88	3.17
Membrane Trafficking R-HSA-199991	2.86	1.77
Signaling By FGFR3 R-HSA-5654741	2.82	5.28
mTORC1-mediated Signaling R-HSA-166208	2.79	7.23
Gene Silencing By RNA R-HSA-211000	2.75	3.07
Signaling By ERBB2 R-HSA-1227986	2.71	4.51
RSK Activation R-HSA-444257	2.69	23.37
FCERI Mediated NF-kB Activation R-HSA-2871837	2.69	3.52
Regulation Of Localization Of FOXO Transcription Factors R-HSA-9614399	2.69	12.53
TICAM1-dependent Activation Of IRF3/IRF7 R-HSA-9013973	2.69	12.53
Inactivation Of CSF3 (G-CSF) Signaling R-HSA-9705462	2.68	6.83
Role Of GTSE1 In G2/M Progression After G2 Checkpoint R-HSA-8852276	2.67	4.03

Term	-log(q-value)	Odds Ratio
Platelet Activation, Signaling And Aggregation R-HSA-76002	2.66	2.19
Interleukin-17 Signaling R-HSA-448424	2.65	3.71
Orc1 Removal From Chromatin R-HSA-68949	2.65	3.71
Signaling By Rho GTPases R-HSA-194315	2.62	1.70
Signaling By SCF-KIT R-HSA-1433557	2.61	4.80
Signaling By Rho GTPases, Miro GTPases And RHOBTB3 R-HSA-9716542	2.61	1.69
Autodegradation Of E3 Ubiquitin Ligase COP1 R-HSA-349425	2.61	4.29
GSK3B And BTRC:CUL1-mediated-degradation Of NFE2L2 R-HSA-9762114	2.61	4.29
Ubiquitin-dependent Degradation Of Cyclin D R-HSA-75815	2.61	4.29
Vpu Mediated Degradation Of CD4 R-HSA-180534	2.61	4.29
Calnexin/calreticulin Cycle R-HSA-901042	2.61	6.47
Infection With Mycobacterium Tuberculosis R-HSA-9635486	2.61	6.47
Dectin-1 Mediated Noncanonical NF-kB Signaling R-HSA-5607761	2.58	3.87
Regulation Of PTEN Gene Transcription R-HSA-8943724	2.58	3.87
Selective Autophagy R-HSA-9663891	2.58	3.87
Regulation Of Apoptosis R-HSA-169911	2.56	4.19
Signaling By Non-Receptor Tyrosine Kinases R-HSA-9006927	2.56	4.19
Chk1/Chk2(Cds1) Mediated Inactivation Of Cyclin B:Cdk1 Complex R-HSA-75035	2.56	10.96
SARS-CoV-2 Targets Host Intracellular Signaling And Regulatory Pathways R-HSA-9755779	2.56	10.96
Suppression Of Phagosomal Maturation R-HSA-9637687	2.56	10.96
TFAP2 (AP-2) Family Regulates Transcription Of Growth Factors And Their Receptors R-HSA-8866910	2.56	10.96
Regulation Of RUNX2 Expression And Activity R-HSA-8939902	2.52	3.52
FLT3 Signaling In Disease R-HSA-9682385	2.52	6.15
Negative Regulators Of DDX58/IFIH1 Signaling R-HSA-936440	2.52	5.21

Term	-log(q-value)	Odds Ratio
Chaperone Mediated Autophagy R-HSA-9613829	2.48	7.52
InlA-mediated Entry Of Listeria Monocytogenes Into Host Cells R-HSA-8876493	2.48	17.53
Cytosolic Sensors Of Pathogen-Associated DNA R-HSA-1834949	2.48	3.72
APC/C:Cdh1 Mediated Degradation Of Cdc20 And APC/C:Cdh1 Targets In Late Mitosis/Early G1 R-HSA-174178	2.48	3.46
TCR Signaling R-HSA-202403	2.48	2.82
Aberrant Regulation Of Mitotic Cell Cycle Due To RB1 Defects R-HSA-9687139	2.45	5.02
FBXL7 Down-Regulates AURKA During Mitotic Entry And In Early Mitosis R-HSA-8854050	2.45	4.00
SCF-beta-TrCP Mediated Degradation Of Emi1 R-HSA-174113	2.45	4.00
Golgi Cisternae Pericentriolar Stack Reorganization R-HSA-162658	2.42	9.74
Prolonged ERK Activation Events R-HSA-169893	2.42	9.74
Regulation Of TP53 Activity Thru Association With Co-factors R-HSA-6804759	2.42	9.74
Hh Mutants Are Degraded By ERAD R-HSA-5362768	2.39	3.91
Deregulated CDK5 Triggers Neurodegenerative Pathways In Alzheimers Disease Models R-HSA-8862803	2.38	7.02
Regulation Of RAS By GAPs R-HSA-5658442	2.38	3.58
Downregulation Of ERBB2 Signaling R-HSA-8863795	2.35	5.59
Negative Regulation Of FGFR3 Signaling R-HSA-5654732	2.35	5.59
Regulation Of TP53 Activity Thru Acetylation R-HSA-6804758	2.35	5.59
DNA Repair R-HSA-73894	2.34	1.97
Activation Of NF-kappaB In B Cells R-HSA-1169091	2.33	3.52
Signaling By NTRKs R-HSA-166520	2.33	2.61
APC/C-mediated Degradation Of Cell Cycle Proteins R-HSA-174143	2.33	3.09
Innate Immune System R-HSA-168249	2.32	1.50
Diseases Of Mitotic Cell Cycle R-HSA-9675126	2.31	4.69

Term	-log(q-value)	Odds Ratio
Assembly Of Pre-Replicative Complex R-HSA-68867	2.31	2.78
Downregulation Of ERBB4 Signaling R-HSA-1253288	2.31	14.02
PTK6 Regulates RTKs And Their Effectors AKT1 And DOK1 R-HSA-8849469	2.31	14.02
Prevention Of Phagosomal-Lysosomal Fusion R-HSA-9636383	2.31	14.02
Regulation Of PTEN Localization R-HSA-8948747	2.31	14.02
Small Interfering RNA (siRNA) Biogenesis R-HSA-426486	2.31	14.02
Activation Of BAD And Translocation To Mitochondria R-HSA-111447	2.31	8.77
IRAK2 Mediated Activation Of TAK1 Complex Upon TLR7/8 Or 9 Stimulation R-HSA-975163	2.31	8.77
Signaling By ERBB4 R-HSA-1236394	2.31	3.74
APC/C:Cdc20 Mediated Degradation Of Securin R-HSA-174154	2.31	3.46
Nuclear Events Mediated By NFE2L2 R-HSA-9759194	2.27	3.20
Hh Mutants Abrogate Ligand Secretion R-HSA-5387390	2.25	3.66
NIK To Noncanonical NF-kB Signaling R-HSA-5676590	2.25	3.66
Switching Of Origins To A Post-Replicative State R-HSA-69052	2.22	2.97
Regulation Of Activated PAK-2p34 By Proteasome Mediated Degradation R-HSA-211733	2.21	3.95
IKK Complex Recruitment Mediated By RIP1 R-HSA-937041	2.21	6.19
Negative Regulation Of PI3K/AKT Network R-HSA-199418	2.21	2.70
Degradation Of GLI1 By Proteasome R-HSA-5610780	2.20	3.59
Degradation Of GLI2 By Proteasome R-HSA-5610783	2.20	3.59
GLI3 Is Processed To GLI3R By Proteasome R-HSA-5610785	2.20	3.59
FOXO-mediated Transcription Of Cell Death Genes R-HSA-9614657	2.18	7.97
TRAF6-mediated Induction Of TAK1 Complex Within TLR4 Complex R-HSA-937072	2.18	7.97
Signaling By NTRK1 (TRKA) R-HSA-187037	2.18	2.67
Interferon Signaling R-HSA-913531	2.17	2.18

Term	-log(q-value)	Odds Ratio
Defective CFTR Causes Cystic Fibrosis R-HSA-5678895	2.15	3.52
Signaling By NOTCH4 R-HSA-9013694	2.15	3.06
Activation Of AP-1 Family Of Transcription Factors R-HSA-450341	2.14	11.68
Growth Hormone Receptor Signaling R-HSA-982772	2.12	5.85
MicroRNA (miRNA) Biogenesis R-HSA-203927	2.12	5.85
Drug-mediated Inhibition Of CDK4/CDK6 Activity R-HSA-9754119	2.12	26.27
RAC3 GTPase Cycle R-HSA-9013423	2.12	2.86
Ubiquitin Mediated Degradation Of Phosphorylated Cdc25A R-HSA-69601	2.11	3.77
RHO GTPase Effectors R-HSA-195258	2.10	1.97
Formation Of Senescence-Associated Heterochromatin Foci (SAHF) R-HSA-2559584	2.07	7.31
Asymmetric Localization Of PCP Proteins R-HSA-4608870	2.06	3.38
Metabolism Of Non-Coding RNA R-HSA-194441	2.06	3.68
RHOD GTPase Cycle R-HSA-9013405	2.06	3.68
UCH Proteinases R-HSA-5689603	2.04	2.79
P75 NTR Receptor-Mediated Signaling R-HSA-193704	2.04	2.79
Cellular Response To Hypoxia R-HSA-1234174	2.04	3.12
RHOC GTPase Cycle R-HSA-9013106	2.04	3.12
Autodegradation Of Cdh1 By Cdh1:APC/C R-HSA-174084	2.01	3.32
Nuclear Import Of Rev Protein R-HSA-180746	2.01	4.55
Vif-mediated Degradation Of APOBEC3G R-HSA-180585	2.01	3.59
TICAM1,TRAF6-dependent Induction Of TAK1 Complex R-HSA-9014325	1.99	10.01
Hedgehog Ligand Biogenesis R-HSA-5358346	1.97	3.26
Oxygen-dependent Proline Hydroxylation Of Hypoxia-inducible Factor Alpha R-HSA-1234176	1.97	3.26
Constitutive Signaling By AKT1 E17K In Cancer R-HSA-5674400	1.96	5.26

Term	-log(q-value)	Odds Ratio
APC/C:Cdc20 Mediated Degradation Of Mitotic Proteins R-HSA-176409	1.96	3.02
N-glycan Trimming In ER And Calnexin/Calreticulin Cycle R-HSA-532668	1.94	4.39
Hedgehog Off State R-HSA-5610787	1.94	2.69
RUNX1 Regulates Transcription Of Genes Involved In Differentiation Of HSCs R-HSA-8939236	1.94	2.69
RAC2 GTPase Cycle R-HSA-9013404	1.93	2.81
Activation Of APC/C And APC/C:Cdc20 Mediated Degradation Of Mitotic Proteins R-HSA-176814	1.92	2.98
CLEC7A (Dectin-1) Signaling R-HSA-5607764	1.91	2.66
Signaling By Hedgehog R-HSA-5358351	1.91	2.37
RUNX1 Regulates Estrogen Receptor Mediated Transcription R-HSA-8931987	1.89	17.51
RUNX1 Regulates Transcription Of Genes Involved In WNT Signaling R-HSA-8939256	1.89	17.51
HSF1-dependent Transactivation R-HSA-3371571	1.89	4.24
Transcriptional Regulation By AP-2 (TFAP2) Family Of Transcription Factors R-HSA-8864260	1.89	4.24
Listeria Monocytogenes Entry Into Host Cells R-HSA-8876384	1.89	6.26
Nuclear Events Stimulated By ALK Signaling In Cancer R-HSA-9725371	1.89	6.26
TICAM1, RIP1-mediated IKK Complex Recruitment R-HSA-168927	1.89	6.26
Mitotic Prophase R-HSA-68875	1.88	2.51
DNA Double-Strand Break Repair R-HSA-5693532	1.87	2.27
Frs2-mediated Activation R-HSA-170968	1.87	8.76
Josephin Domain DUBs R-HSA-5689877	1.87	8.76
ER-Phagosome Pathway R-HSA-1236974	1.87	2.74
Platelet Degranulation R-HSA-114608	1.85	2.40
DNA Damage Recognition In GG-NER R-HSA-5696394	1.83	4.10
Interactions Of Rev With Host Cellular Proteins R-HSA-177243	1.83	4.10
Recycling Pathway Of L1 R-HSA-437239	1.83	4.78

Term	-log(q-value)	Odds Ratio
ABC-family Proteins Mediated Transport R-HSA-382556	1.82	2.57
Apoptotic Factor-Mediated Response R-HSA-111471	1.80	5.84
Signal Transduction By L1 R-HSA-445144	1.80	5.84
Signaling By Hippo R-HSA-2028269	1.80	5.84
DNA Replication Pre-Initiation R-HSA-69002	1.80	2.36
Regulation Of APC/C Activators Between G1/S And Early Anaphase R-HSA-176408	1.78	2.80
RHOB GTPase Cycle R-HSA-9013026	1.78	2.98
Antigen processing-Cross Presentation R-HSA-1236975	1.77	2.51
Disassembly Of Destruction Complex And Recruitment Of AXIN To Membrane R-HSA-4641262	1.77	4.58
HSF1 Activation R-HSA-3371511	1.77	4.58
Processing Of Capped Intronless Pre-mRNA R-HSA-75067	1.77	4.58
Adenylate Cyclase Inhibitory Pathway R-HSA-170670	1.76	7.79
Cytochrome C-Mediated Apoptotic Response R-HSA-111461	1.76	7.79
NF-kB Is Activated And Signals Survival R-HSA-209560	1.76	7.79
DDX58/IFIH1-mediated Induction Of Interferon-Alpha/Beta R-HSA-168928	1.76	2.76
EPH-ephrin Mediated Repulsion Of Cells R-HSA-3928665	1.73	3.43
ER Quality Control Compartment (ERQC) R-HSA-901032	1.72	5.48
Response To Elevated Platelet Cytosolic Ca2+ R-HSA-76005	1.72	2.30
Global Genome Nucleotide Excision Repair (GG-NER) R-HSA-5696399	1.72	2.72
FLT3 Signaling By CBL Mutants R-HSA-9706377	1.71	13.13
Modulation By Mtb Of Host Immune System R-HSA-9637628	1.71	13.13
Transcriptional Regulation By MECP2 R-HSA-8986944	1.71	3.10
Diseases Of Programmed Cell Death R-HSA-9645723	1.71	2.88
PI5P, PP2A And IER3 Regulate PI3K/AKT Signaling R-HSA-6811558	1.71	2.46

Term	-log(q-value)	Odds Ratio
MAPK Targets/ Nuclear Events Mediated By MAP Kinases R-HSA-450282	1.71	4.39
Separation Of Sister Chromatids R-HSA-2467813	1.69	2.09
RHO GTPases Activate Formins R-HSA-5663220	1.69	2.35
Signaling By FGFR4 R-HSA-5654743	1.68	3.72
CDK-mediated Phosphorylation And Removal Of Cdc6 R-HSA-69017	1.68	2.83
Cdc20:Phospho-APC/C Mediated Degradation Of Cyclin A R-HSA-174184	1.68	2.83
AKT Phosphorylates Targets In Cytosol R-HSA-198323	1.66	7.01
Nucleotide Excision Repair R-HSA-5696398	1.65	2.41
Signaling By NODAL R-HSA-1181150	1.65	5.16
Negative Regulation Of FGFR4 Signaling R-HSA-5654733	1.65	4.21
Regulation Of MECP2 Expression And Activity R-HSA-9022692	1.65	4.21
APC:Cdc20 Mediated Degradation Of Cell Cycle Proteins Before Cycle Checkpoint Satisfied R-HSA-179419	1.64	2.79
Pre-NOTCH Transcription And Translation R-HSA-1912408	1.63	2.98
Negative Regulation Of MAPK Pathway R-HSA-5675221	1.63	3.61
Hedgehog On State R-HSA-5632684	1.63	2.61
Potential Therapeutics For SARS R-HSA-9679191	1.62	2.48
Rab Regulation Of Trafficking R-HSA-9007101	1.61	2.28
Cell Death Signaling Via NRAGE, NRIF And NADE R-HSA-204998	1.61	2.75
Apoptotic Execution Phase R-HSA-75153	1.60	3.19
Signaling By MET R-HSA-6806834	1.60	2.93
Signaling By FGFR R-HSA-190236	1.60	2.58
Nuclear Signaling By ERBB4 R-HSA-1251985	1.59	4.05
Formation Of Incision Complex In GG-NER R-HSA-5696395	1.58	3.51
Late Phase Of HIV Life Cycle R-HSA-162599	1.58	2.18

Term	-log(q-value)	Odds Ratio
HIV Life Cycle R-HSA-162587	1.58	2.12
Regulation Of PLK1 Activity At G2/M Transition R-HSA-2565942	1.57	2.54
InlB-mediated Entry Of Listeria Monocytogenes Into Host Cell R-HSA-8875360	1.57	6.37
Regulation Of Innate Immune Responses To Cytosolic DNA R-HSA-3134975	1.57	6.37
Signaling By FLT3 ITD And TKD Mutants R-HSA-9703648	1.57	6.37
Myoclonic Epilepsy Of Lafora R-HSA-3785653	1.57	10.51
RUNX2 Regulates Genes Involved In Cell Migration R-HSA-8941332	1.57	10.51
Recycling Of eIF2:GDP R-HSA-72731	1.57	10.51
Transcriptional Regulation By Small RNAs R-HSA-5578749	1.54	2.66
Protein Localization R-HSA-9609507	1.54	2.04
Cooperation Of Prefoldin And TriC/CCT In Actin And Tubulin Folding R-HSA-389958	1.54	3.90
Negative Regulation Of FGFR1 Signaling R-HSA-5654726	1.54	3.90
Mitochondrial Protein Import R-HSA-1268020	1.53	2.82
Aggrephagy R-HSA-9646399	1.52	4.61
RUNX2 Regulates Osteoblast Differentiation R-HSA-8940973	1.52	4.61
Death Receptor Signaling R-HSA-73887	1.51	2.13
ABC Transporter Disorders R-HSA-5619084	1.51	2.62
Unfolded Protein Response (UPR) R-HSA-381119	1.51	2.48

Table 3. *List of unique pathways from Reactome derived from up-regulated predicted mRNA target in high-sodium diet*

Table 4

Term	-log(q-value)	Odds Ratio
TP53 Regulates Transcription Of Genes Involved In G1 Cell Cycle Arrest R-HSA-6804116	3.11	14.21
TP53 Regulates Transcription Of Cell Cycle Genes R-HSA-6791312	2.54	4.62
Activation Of HOX Genes During Differentiation R-HSA-5619507	2.44	3.28
Signaling By Erythropoietin R-HSA-9006335	2.40	7.11
Transcriptional Regulation Of White Adipocyte Differentiation R-HSA-381340	2.39	3.36
Signaling By PDGF R-HSA-186797	2.37	4.27
Nuclear Receptor Transcription Pathway R-HSA-383280	2.31	4.17
Ca2+ Pathway R-HSA-4086398	2.30	3.86
Constitutive Signaling By EGFRvIII R-HSA-5637810	2.28	10.65
Neddylation R-HSA-8951664	2.15	2.15
Signaling By ERBB2 ECD Mutants R-HSA-9665348	2.10	9.47
RNA Polymerase II Transcribes snRNA Genes R-HSA-6807505	2.03	3.32
Golgi-to-ER Retrograde Transport R-HSA-8856688	1.95	2.73
RUNX3 Regulates CDKN1A Transcription R-HSA-8941855	1.83	18.91
Nuclear Envelope Breakdown R-HSA-2980766	1.82	3.73
Phospholipid Metabolism R-HSA-1483257	1.82	2.13
Pyruvate Metabolism And Citric Acid (TCA) Cycle R-HSA-71406	1.78	3.64
Pyruvate Metabolism R-HSA-70268	1.77	4.94
Constitutive Signaling By Ligand-Responsive EGFR Cancer Variants R-HSA-1236382	1.75	7.10
JNK (c-Jun Kinases) Phosphorylation And Activation Mediated By Activated Human TAK1 R-HSA-450321	1.75	7.10
Signaling By ALK Fusions And Activated Point Mutants R-HSA-9725370	1.74	3.56
Erythropoietin Activates RAS R-HSA-9027284	1.67	8.87

Signaling By PDGFR In Disease R-HSA-9671555	1.67	6.55
SHC-related Events Triggered By IGF1R R-HSA-2428933	1.67	14.18
SUMOylation Of Chromatin Organization Proteins R-HSA-4551638	1.66	3.40
Metabolism Of Lipids R-HSA-556833	1.65	1.52
COPI-independent Golgi-to-ER Retrograde Traffic R-HSA-6811436	1.59	4.37
Postmitotic Nuclear Pore Complex (NPC) Reformation R-HSA-9615933	1.57	4.97
Role Of LAT2/NTAL/LAB On Calcium Mobilization R-HSA-2730905	1.57	7.88
Triglyceride Biosynthesis R-HSA-75109	1.57	7.88
PPARA Activates Gene Expression R-HSA-1989781	1.56	2.45
Fcgamma Receptor (FCGR) Dependent Phagocytosis R-HSA-2029480	1.56	2.73
SUMOylation Of Transcription Cofactors R-HSA-3899300	1.54	3.76
CD163 Mediating An Anti-Inflammatory Response R-HSA-9662834	1.52	11.34
MET Promotes Cell Motility R-HSA-8875878	1.51	4.73
Regulation Of Lipid Metabolism By PPARalpha R-HSA-400206	1.51	2.40
Intra-Golgi And Retrograde Golgi-to-ER Traffic R-HSA-6811442	1.51	2.08
Interleukin-3, Interleukin-5 And GM-CSF Signaling R-HSA-512988	1.50	3.65
Platelet Aggregation (Plug Formation) R-HSA-76009	1.50	4.06

Table 4. *List of unique pathways from Reactome derived from up-regulated predicted mRNA target in low-sodium diet*

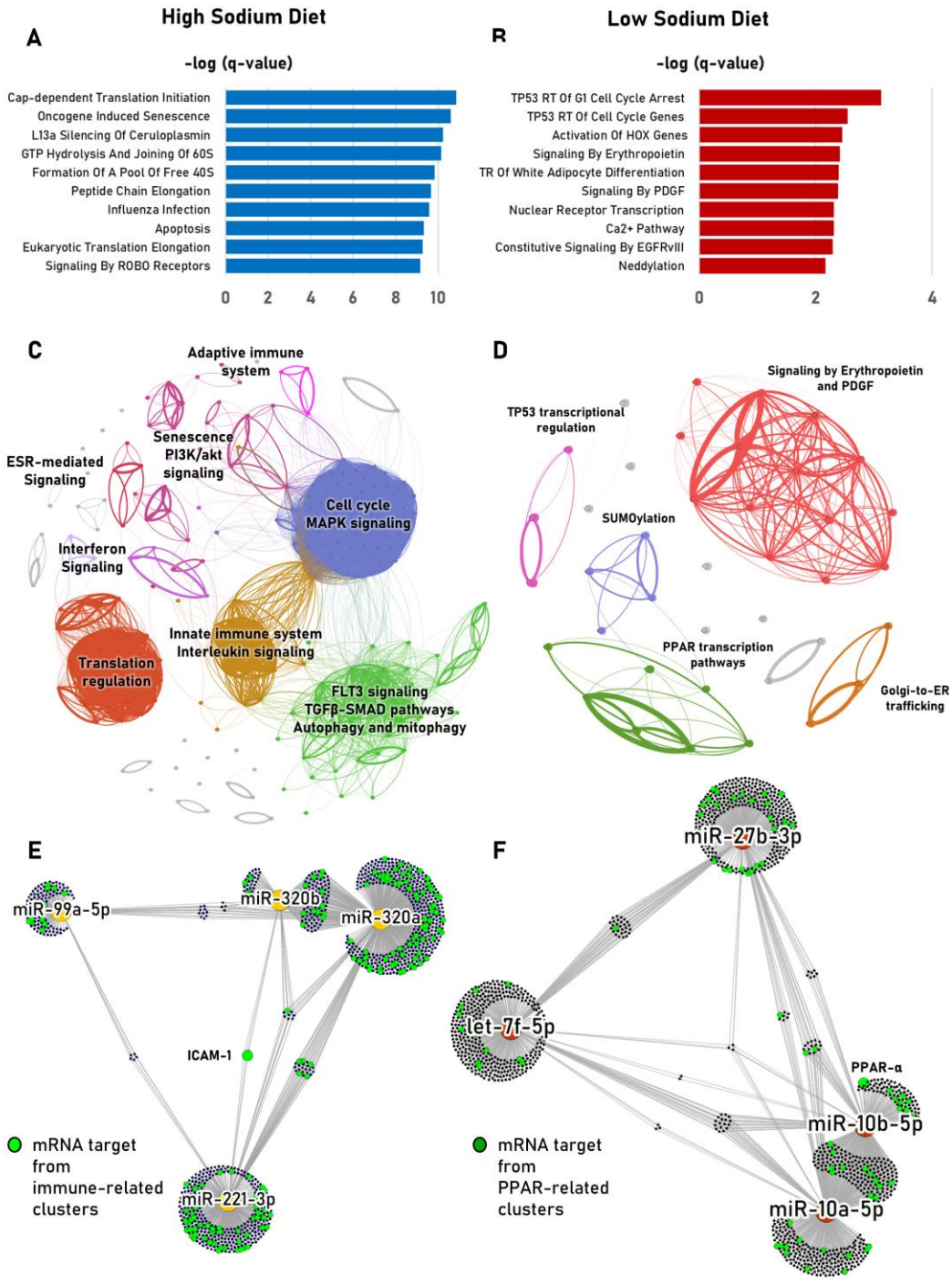

Figure 4. Bioinformatic network analysis of predicted differentially regulated mRNA targets of differentially enriched miRNAs. *(A-B) Pathway enrichment analysis conducted with EnrichR showing the enriched terms for miRNA target genes upregulated in high sodium diet (A) or in low sodium diet (B). Adjustment of*

p-value was performed with Benjamini-Hochberg to calculate q-values; the -log(q value) was calculated for pathway bar graph and network analysis. Pathways uniquely enriched in each condition were considered for pathway and network analysis. (C-D) Network cluster analysis showing pathways enriched in high (C) and low sodium diet (D). The node size is proportional to -log(q-value) of each pathway. For clarity of representation, pathways with -log(q-value)< 1.5 were excluded in "low sodium diet" network and -log(q-value)< 2.0 in "high sodium diet". Connection thickness is proportional to the Jaccard Index. The main functional communities were named on the basis of the principal enriched pathways for each cluster. (E-F) miRNA-mRNA target networks showing miRNA-target interactions in high (E) and low sodium diet (F). Yellow dots indicate miR down-regulated in high sodium diet (E) and red dots in low sodium diet (F); blue dots indicate mRNA targets and are connected to regulating miRNAs. mRNA targets involved in "immune-related clusters" (adaptive immune system, innate immune system-interleukin signaling and interferon signaling) are highlighted in green in high sodium diet (E). mRNA targets involved in "PPAR-related clusters" highlighted in green in low sodium diet (F). In HSD (E), the connection between miR-320b and ICAM-1, was added manually since validated by one previously published study[24].

3.4 *miRNA-mRNA target networks*

To identify potential miRNA-mRNA target responsible for the effects of HSD at kidney level, we built new miRNA-mRNA target networks specific. In these networks, each differentially expressed miRNA was connected to predicted and validated mRNA target. Considering that previous pre-clinical studies suggested that low-grade renal inflammation may favor the development of salt-sensitive hypertension [25], we leveraged the miRNA-mRNA target networks for the detection of mRNA targets involved in immune system regulation. In HSD, we highlighted mRNA targets involved in immune-related clusters (adaptive immune system, innate immune system-interleukin signaling and interferon signaling) (Figure 4E). Considering the anti-inflammatory role of PPARα at renal level[26], we highlighted mRNA target involved in PPAR transcription cluster in LSD (Figure 4F). mRNA targets related to immune system regulation were uniformly connected to all the

miRNAs differentially expressed in both dietary conditions, suggesting that the enrichment of these pathways was not exclusive of one or few miRNAs. Hence, we identified two potential mRNA targets in high and LSD, as candidates for *in vitro* validation. Intercellular adhesion molecule 1 (*ICAM-1*) (Figure 4E) is a validated target of miR-221 in human cholangiocytes[27] and of miR-320b in human endothelial cells[24] (although this last validation was not present in MiRTarBase). *PPARα*, which is predicted as upregulated in LSD (Figure 4F), is a validated target of miR-10b in human hepatocytes[28].

3.5 *In vitro validation*

Since both *ICAM-1* and *PPARα* were validated as mRNA targets in non-renal cells, we designed a proof-of-concept *in vitro* validation of both mRNA targets in human proximal tubular cell line (HK-2 cells). The transfection of miR-320b inhibitor in HK-2 cells resulted in an efficient knockdown of miR-320b (Figure 5A), 2.17-fold increase of *ICAM-1* mRNA expression (Figure 5B) and 2.21-fold increase in *ICAM-1* protein (Figure 5C), as assessed by flow-cytometry. The transfection of miR-10b-5p inhibitor in the same cells resulted in an efficient knockdown of miR-10b-5p (Figure 5D), non-significant modification of *PPAR-α* mRNA (Figure 5E), but 2.85-fold increase in PPAR-α protein (Figure 5F –Figure 6), assessed by Western Blot analysis.

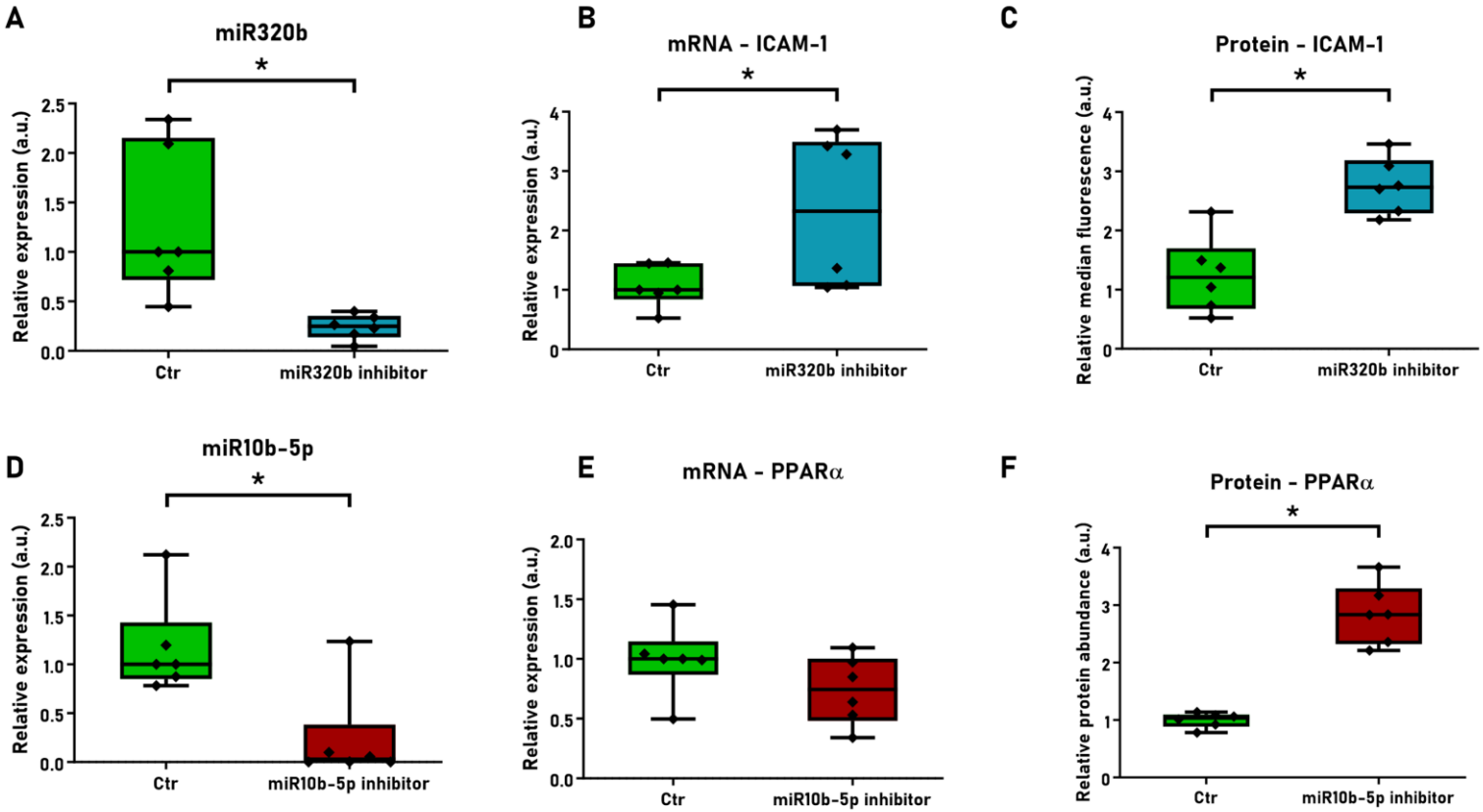

Figure 5. In vitro validation of miRNA-target regulation in human proximal tubular cell lines (HK-2 cells). *(A-C) Relative expression levels of miR-320b (A), mRNA of intercellular adhesion molecule 1 (ICAM-1) (B), and protein levels of ICAM-1 (C) in HK-2 cells after*

*treatment with miR-320b inhibitor. (D-F) Relative expression levels of miR-10b-5p (D), mRNA of peroxisome proliferator-activated receptor α (PPARα) (E), and protein levels of PPARα (F) in HK-2 cells after treatment with miR-10b-5p inhibitor. Expression levels were normalized to miR-16-5p expression (arbitrary unit (a.u.)) for miRNAs, to glyceraldehyde 3-phosphate dehydrogenase (GAPDH) expression (a.u.) for mRNA. Protein abundance was normalized for vinculin expression (a.u.). (A, B D, and E) were quantified by quantitative real-time polymerase chain reaction (qRT-PCR), median fluorescence of each experiment was normalized by z-score (a.u.). (C and F) Protein expression was quantified by Western Blot. Representative western blot analysis of PPARα and vinculin is presented in Figure 6. In all the experiments the control group was treated with the empty vehicle (Lipofectamine 2000) alone. Data are represented with dot plots. Each experiment was repeated twice with 3 technical replicates (n=6). Statistical differences were assessed by the use unpaired t-test. *P<0.05*

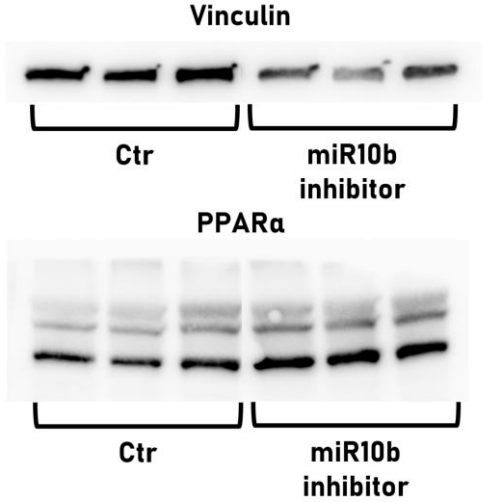

Figure 4. Western Blot analyses of PPARα protein abundance in HK-2 cells treated with miR-10b-5p inhibitor. *Representative Western blot analysis of PPARα and vinculin, comparing protein expression of PPARα after mR-10b-5p inhibition.*

4. DISCUSSION

The uEVs hold significant potential for several research fields, due to their non-invasive collection method, their role as carriers of bioactive molecules, and their ability to reflect the physiological and pathological state of the urinary tract.

Taking advantage of a strict dietary sodium manipulation, achieved by providing participants with low sodium and high sodium meals, we investigated for the first time the potential impact of dietary sodium levels on the small-RNAome of uEVs isolated from high-risk normotensive subjects. In total, 8 miRNAs were differentially expressed in the 2 dietary conditions. Interestingly, these miRNAs were targeting genes that after bioinformatic analysis, were enriched into pathways related to immune system activation in HSD and anti-inflammatory pathways in LSD. We hence validated the miRNA-mRNA targets of interest *in vitro* in human proximal tubular cells, showing miR-320b regulation of *ICAM-1* and miR-10b-5p regulation of *PPARα*.

In the last three decades, the results of pre-clinical studies supported the hypothesis that sodium excess induces hypertension through several mechanisms that go beyond the mere hemodynamic effects[8,9]. The relationship between HSD and cardiovascular risk involves a multiple arrays of pathways, including ageing, endothelial dysfunction, redox signaling and immune system activation[8,29]. In animal models, sodium excess is able to stimulate systemic innate immune response, with increased circulating neutrophils[30], monocytes [30,31] and the activation of antigen presenting cells (APCs)[32]. Activated APCs polarize T cells towards an interleukin-17 (IL-17) producing phenotype, with the activation of

adaptive immune system and migration of inflammatory cells to target organs[9,33]. In the present study, the miRNA set found altered following HSD was connected with a series of gene targets that in a network analysis showed an enrichment of both adaptive and innate immune system regulation, corroborating the findings from animal models after high sodium intake[9,30,33]. Moreover, we showed significant enrichment of pathways related to interferon signaling, whose role in high sodium condition has been previously investigated in a murine model, where sodium excess stimulates interferon γ (IFNγ) secreting T regulatory cells with consequent pro-inflammatory action[34].

In Dahl salt-sensitive rats[35] and in another murine model[36], the sodium load induces significant infiltration of T lymphocytes into the kidney that is followed by hypertension and development of renal disease[35]. The examination of human kidneys from hypertensive patients, showed an accumulation of monocyte, macrophage, and dendritic cells in the corticomedullary junction and into the deeper regions of medulla, where sodium concentrations are markedly increased [37]. The local complex interplay between innate and adaptive immunity further stimulates the pro-inflammatory milieu induced by sodium excess[34]. Infiltration of inflammatory cells in the kidney is therefore crucial for the development of low-grade renal inflammation induced by sodium.

In this study, we showed that miR-320b is down-regulated in uEVs after HSD and miR-320b inhibition increases *ICAM-1* mRNA and protein expression, in human tubular cell line. In the kidney, *ICAM-1* is expressed in the renal vascular endothelium and in proximal tubular epithelium, especially under pathological

stimuli[38,39], and is associated with interstitial infiltration of inflammatory cells[38,40]. In Dahl salt-sensitive rats, the administration of HSD increases leukocyte adhesion and the renal expression of monocyte chemotactic protein-1 (MCP-1) and ICAM-1[33], through mechanisms that are independent from sodium-induced hypertension[33]. Moreover, *ICAM-1* expression is induced by IFNγ[27]. Considering that we identified enrichment of interferon signaling after HSD, we can speculate that multiple mechanisms can synergize, increasing ICAM-1 at renal level after sodium load.

In LSD, the miRNAs altered were targeting a set of genes enriched in pathways related to white adipocyte differentiation and *PPAR* transcriptional regulation. In the kidney, PPARα is expressed in medullary thick ascending limbs and the proximal tubular epithelium where it plays a critical role in metabolic regulation and anti-inflammatory activity[26]. In a transgenic mouse model, the increased expression of proximal tubule PPARα reduced adhesion molecules, pro-inflammatory cytokines, and the infiltration of inflammatory mononuclear cells[41]. On the other side, diabetic PPARα-knockout mice display increased renal macrophage infiltration and more severe diabetic renal disease than diabetic wild-type mice[42]. In our study, we showed that miR-10b-5p was down-regulated after LSD and that this miRNA inhibition increases the expression of PPARα protein in human proximal tubular cells, potentially contributing to the anti-inflammatory pathways of LSD. It should be noticed that miR-10b-5p inhibition increased PPARα protein, without significant modification of PPARα mRNA. This finding is consistent with the results of one previous study, that showed that miR-10b

regulates PPARα post-transcriptionally in human hepatocytes, without significant modification of mRNA levels[28].

Beyond the anti-inflammatory effects, PPARα have also nephroprotective properties through regulation of renal fibrosis[41]. In particular, PPARα reduces tubulointerstitial fibrosis through reduction of proximal tubule expression of TGFβ[41]. Intriguingly, in our study, several TGFβ-related pathways were enriched in HSD. We can speculate that a relative reduction of PPARα activity in HSD can further enhance TGFβ activation leading to interstitial fibrosis with sodium excess.

pRNAs (PIWI-interacting RNAs) are small non-coding RNAs of 23-31 nucleotides which bind to PIWI-clade members of the Argonaute protein family[43]. Unlike miRNAs, piRNAs are generated by cleavage of single stranded transcripts. The most known and described role of piRNAs is to silence transposable elements (or transposons) in germ cells. PIWI-piRNA dysregulation has been associated with inferitility, cancer diseases and neurodegenerative diseases. Emerging findings suggest that piRNAs may have a role in somatic cells of liver, heart, peripheral blood cells and pancreatic β cells[44]. However, the comprehension of the role of piRNAs in somatic cells is still preliminary. Bionformatic analysis of piRNA predicted targets[45] showed that two differentially enriched piRNAs can regulate genes involved in renal fibrosis and hypertension at renal level. In details, Fibroblast Growth Factor 5 (FGF5) and GLI Family Zinc Finger 1 (GLI1) are predicted targets of piR-23574 and piR-32159 respectively[45]. FGF5 polymorphisms have been associated with hypertension and increased cardiovascular risk[46] and other Fibroblast Growth Factors have been described as contributors to blood

pressure regulation through renal pathways[47]. GLI1-expressing mesenchymal cells, instead, showed a potential role in kidney damage by induction of renal fibrosis[48].

5. CONCLUSIONS

The analysis of the small-RNAome of human uEVs revealed that HSD induces the activation of pro-inflammatory pathways that potentially contribute to the development of hypertension and kidney damage. Our findings unravel an important role of miRNA in the regulation of critical gene targets, with up-regulation of *ICAM-1* in HSD and up-regulation of *PPARα* in LSD.

6. REFERENCES

1. Chen X, Du J, Wu X, Cao W, Sun S. Global burden attributable to high sodium intake from 1990 to 2019. *Nutr Metab Cardiovasc Dis*. 2021;31(12):3314-3321. doi:10.1016/j.numecd.2021.08.033

2. Campbell NRC, Whelton PK, Orias M, Wainford RD, Cappuccio FP, Ide N, Neal B, Cohn J, Cobb LK, Webster J, Trieu K, He FJ, McLean RM, Blanco-Metzler A, Woodward M, Khan N, Kokubo Y, Nederveen L, Arcand J, MacGregor GA, Owolabi MO, Lisheng L, Parati G, Lackland DT, Charchar FJ, Williams B, Tomaszewski M, Romero CA, Champagne B, L'Abbe MR, Weber MA, Schlaich MP, Fogo A, Feigin VL, Akinyemi R, Inserra F, Menon B, Simas M, Neves MF, Hristova K, Pullen C, Pandeya S, Ge J, Jalil JE, Wang JG, Wideimsky J, Kreutz R, Wenzel U, Stowasser M, Arango M, Protogerou A, Gkaliagkousi E, Fuchs FD, Patil M, Chan AWK, Nemcsik J, Tsuyuki RT, Narasingan SN, Sarrafzadegan N, Ramos ME, Yeo N, Rakugi H, Ramirez AJ, Álvarez G, Berbari A, Kim CI, Ihm SH, Chia YC, Unurjargal T, Park HK, Wahab K, McGuire H, Dashdorj NJ, Ishaq M, Ona DID, Mercado-Asis LB, Prejbisz A, Leenaerts M, Simão C, Pinto F, Almustafa BA, Spaak J, Farsky S, Lovic D, Zhang XH. 2022 World Hypertension League, Resolve To Save Lives and International Society of Hypertension dietary sodium (salt) global call to action. *J Hum Hypertens*. Published online May 17, 2022:1-10. doi:10.1038/s41371-022-00690-0

3. Mente A, O'Donnell M, Rangarajan S, Dagenais G, Lear S, McQueen M, Diaz R, Avezum A, Lopez-Jaramillo P, Lanas F, Li W, Lu Y, Yi S, Rensheng L, Iqbal R, Mony P, Yusuf R, Yusoff K, Szuba A, Oguz A, Rosengren A, Bahonar A, Yusufali A, Schutte AE, Chifamba J, Mann JFE, Anand SS, Teo K, Yusuf S, PURE, EPIDREAM and ONTARGET/TRANSCEND Investigators. Associations of urinary sodium excretion with cardiovascular events in individuals with and without hypertension: a pooled analysis of data from four studies. *Lancet*. 2016;388(10043):465-475. doi:10.1016/S0140-6736(16)30467-6

4. Filippini T, Malavolti M, Whelton PK, Naska A, Orsini N, Vinceti M. Blood Pressure Effects of Sodium Reduction: Dose-Response Meta-Analysis of Experimental Studies. *Circulation*. 2021;143(16):1542-1567. doi:10.1161/CIRCULATIONAHA.120.050371

5. Aburto NJ, Ziolkovska A, Hooper L, Elliott P, Cappuccio FP, Meerpohl JJ. Effect of lower sodium intake on health: systematic review and meta-analyses. *BMJ*. 2013;346:f1326. doi:10.1136/bmj.f1326

6. Piepoli MF, Hoes AW, Agewall S, Albus C, Brotons C, Catapano AL, Cooney MT, Corrà U, Cosyns B, Deaton C, Graham I, Hall MS, Hobbs FDR, Løchen ML, Löllgen H, Marques-Vidal P, Perk J, Prescott E, Redon J, Richter DJ, Sattar N, Smulders Y, Tiberi M, van der Worp HB, van Dis I, Verschuren WMM, Binno S, ESC Scientific Document Group. 2016 European Guidelines on cardiovascular disease prevention in clinical practice: The Sixth Joint Task Force of the European Society of Cardiology and Other Societies on Cardiovascular Disease Prevention in Clinical Practice (constituted by representatives of 10 societies and by invited experts)Developed with the special contribution of the European Association for

Cardiovascular Prevention & Rehabilitation (EACPR). *Eur Heart J*. 2016;37(29):2315-2381. doi:10.1093/eurheartj/ehw106

7. Mancia Chairperson G, Kreutz Co-Chair R, Brunström M, Burnier M, Grassi G, Januszewicz A, Muiesan ML, Tsioufis K, Agabiti-Rosei E, Algharably EAE, Azizi M, Benetos A, Borghi C, Hitij JB, Cifkova R, Coca A, Cornelissen V, Cruickshank K, Cunha PG, Danser AHJ, de Pinho RM, Delles C, Dominiczak AF, Dorobantu M, Doumas M, Fernández-Alfonso MS, Halimi JM, Járai Z, Jelaković B, Jordan J, Kuznetsova T, Laurent S, Lovic D, Lurbe E, Mahfoud F, Manolis A, Miglinas M, Narkiewicz K, Niiranen T, Palatini P, Parati G, Pathak A, Persu A, Polonia J, Redon J, Sarafidis P, Schmieder R, Spronck B, Stabouli S, Stergiou G, Taddei S, Thomopoulos C, Tomaszewski M, Van de Borne P, Wanner C, Weber T, Williams B, Zhang ZY, Kjeldsen SE, Authors/Task Force Members: 2023 ESH Guidelines for the management of arterial hypertension The Task Force for the management of arterial hypertension of the European Society of Hypertension Endorsed by the European Renal Association (ERA) and the International Society of Hypertension (ISH). *J Hypertens*. Published online June 21, 2023. doi:10.1097/HJH.0000000000003480

8. Afsar B, Kuwabara M, Ortiz A, Yerlikaya A, Siriopol D, Covic A, Rodriguez-Iturbe B, Johnson RJ, Kanbay M. Salt Intake and Immunity. *Hypertension*. 2018;72(1):19-23. doi:10.1161/HYPERTENSIONAHA.118.11128

9. Elijovich F, Kleyman TR, Laffer CL, Kirabo A. Immune Mechanisms of Dietary Salt-Induced Hypertension and Kidney Disease: Harry Goldblatt Award for Early Career Investigators 2020. *Hypertension*. 2021;78(2):252-260. doi:10.1161/HYPERTENSIONAHA.121.16495

10. van Niel G, D'Angelo G, Raposo G. Shedding light on the cell biology of extracellular vesicles. *Nat Rev Mol Cell Biol*. 2018;19(4):213-228. doi:10.1038/nrm.2017.125

11. Crescitelli R, Lässer C, Jang SC, Cvjetkovic A, Malmhäll C, Karimi N, Höög JL, Johansson I, Fuchs J, Thorsell A, Gho YS, Olofsson Bagge R, Lötvall J. Subpopulations of extracellular vesicles from human metastatic melanoma tissue identified by quantitative proteomics after optimized isolation. *J Extracell Vesicles*. 2020;9(1):1722433. doi:10.1080/20013078.2020.1722433

12. Pardini B, Calin GA. MicroRNAs and Long Non-Coding RNAs and Their Hormone-Like Activities in Cancer. *Cancers (Basel)*. 2019;11(3):378. doi:10.3390/cancers11030378

13. Barros ER, Carvajal CA. Urinary Exosomes and Their Cargo: Potential Biomarkers for Mineralocorticoid Arterial Hypertension? *Front Endocrinol (Lausanne)*. 2017;8:230. doi:10.3389/fendo.2017.00230

14. Erdbrügger U, Blijdorp CJ, Bijnsdorp IV, Borràs FE, Burger D, Bussolati B, Byrd JB, Clayton A, Dear JW, Falcón-Pérez JM, Grange C, Hill AF, Holthöfer H, Hoorn EJ, Jenster G, Jimenez CR, Junker K, Klein J, Knepper MA, Koritzinsky EH, Luther JM, Lenassi M, Leivo J, Mertens I, Musante L, Oeyen E, Puhka M, van Royen ME, Sánchez C, Soekmadji C, Thongboonkerd V, van Steijn V, Verhaegh

G, Webber JP, Witwer K, Yuen PST, Zheng L, Llorente A, Martens-Uzunova ES. Urinary extracellular vesicles: A position paper by the Urine Task Force of the International Society for Extracellular Vesicles. *J Extracell Vesicles*. 2021;10(7):e12093. doi:10.1002/jev2.12093

15. Huntzinger E, Izaurralde E. Gene silencing by microRNAs: contributions of translational repression and mRNA decay. *Nat Rev Genet*. 2011;12(2):99-110. doi:10.1038/nrg2936

16. Bustin SA, Benes V, Garson JA, Hellemans J, Huggett J, Kubista M, Mueller R, Nolan T, Pfaffl MW, Shipley GL, Vandesompele J, Wittwer CT. The MIQE guidelines: minimum information for publication of quantitative real-time PCR experiments. *Clin Chem*. 2009;55(4):611-622. doi:10.1373/clinchem.2008.112797

17. Sabo AA, Birolo G, Naccarati A, Dragomir MP, Aneli S, Allione A, Oderda M, Allasia M, Gontero P, Sacerdote C, Vineis P, Matullo G, Pardini B. Small Non-Coding RNA Profiling in Plasma Extracellular Vesicles of Bladder Cancer Patients by Next-Generation Sequencing: Expression Levels of miR-126-3p and piR-5936 Increase with Higher Histologic Grades. *Cancers (Basel)*. 2020;12(6):1507. doi:10.3390/cancers12061507

18. Martin M. Cutadapt removes adapter sequences from high-throughput sequencing reads. *EMBnet.journal*. 2011;17(1):10-12. doi:10.14806/ej.17.1.200

19. Li H. Exploring single-sample SNP and INDEL calling with whole-genome de novo assembly. *Bioinformatics*. 2012;28(14):1838-1844. doi:10.1093/bioinformatics/bts280

20. Love MI, Huber W, Anders S. Moderated estimation of fold change and dispersion for RNA-seq data with DESeq2. *Genome Biol*. 2014;15(12):550. doi:10.1186/s13059-014-0550-8

21. Huang HY, Lin YCD, Li J, Huang KY, Shrestha S, Hong HC, Tang Y, Chen YG, Jin CN, Yu Y, Xu JT, Li YM, Cai XX, Zhou ZY, Chen XH, Pei YY, Hu L, Su JJ, Cui SD, Wang F, Xie YY, Ding SY, Luo MF, Chou CH, Chang NW, Chen KW, Cheng YH, Wan XH, Hsu WL, Lee TY, Wei FX, Huang HD. miRTarBase 2020: updates to the experimentally validated microRNA-target interaction database. *Nucleic Acids Res*. 2020;48(D1):D148-D154. doi:10.1093/nar/gkz896

22. Xie Z, Bailey A, Kuleshov MV, Clarke DJB, Evangelista JE, Jenkins SL, Lachmann A, Wojciechowicz ML, Kropiwnicki E, Jagodnik KM, Jeon M, Ma'ayan A. Gene Set Knowledge Discovery with Enrichr. *Curr Protoc*. 2021;1(3):e90. doi:10.1002/cpz1.90

23. Blondel VD, Guillaume JL, Lambiotte R, Lefebvre E. Fast unfolding of communities in large networks. *J Stat Mech*. 2008;2008(10):P10008. doi:10.1088/1742-5468/2008/10/P10008

24. Gidlöf O, van der Brug M, Ohman J, Gilje P, Olde B, Wahlestedt C, Erlinge D. Platelets activated during myocardial infarction release functional miRNA, which

can be taken up by endothelial cells and regulate ICAM1 expression. *Blood*. 2013;121(19):3908-3917, S1-26. doi:10.1182/blood-2012-10-461798

25. Lu X, Crowley SD. Inflammation in Salt-Sensitive Hypertension and Renal Damage. *Curr Hypertens Rep*. 2018;20(12):103. doi:10.1007/s11906-018-0903-x

26. Gao J, Gu Z. The Role of Peroxisome Proliferator-Activated Receptors in Kidney Diseases. *Front Pharmacol*. 2022;13:832732. doi:10.3389/fphar.2022.832732

27. Hu G, Gong AY, Liu J, Zhou R, Deng C, Chen XM. miR-221 suppresses ICAM-1 translation and regulates interferon-gamma-induced ICAM-1 expression in human cholangiocytes. *Am J Physiol Gastrointest Liver Physiol*. 2010;298(4):G542-550. doi:10.1152/ajpgi.00490.2009

28. Zheng L, Lv G cai, Sheng J, Yang Y da. Effect of miRNA-10b in regulating cellular steatosis level by targeting PPAR-alpha expression, a novel mechanism for the pathogenesis of NAFLD. *J Gastroenterol Hepatol*. 2010;25(1):156-163. doi:10.1111/j.1440-1746.2009.05949.x

29. Pilic L, Pedlar CR, Mavrommatis Y. Salt-sensitive hypertension: mechanisms and effects of dietary and other lifestyle factors. *Nutr Rev*. 2016;74(10):645-658. doi:10.1093/nutrit/nuw028

30. Shen K, DeLano FA, Zweifach BW, Schmid-Schönbein GW. Circulating leukocyte counts, activation, and degranulation in Dahl hypertensive rats. *Circ Res*. 1995;76(2):276-283. doi:10.1161/01.res.76.2.276

31. Artigues C, Richard V, Roussel C, Lallemand F, Henry JP, Thuillez C. Increased endothelium--monocyte interactions in salt-sensitive hypertension: effect of L-arginine. *J Cardiovasc Pharmacol*. 2000;35(3):468-473. doi:10.1097/00005344-200003000-00018

32. Barbaro NR, Foss JD, Kryshtal DO, Tsyba N, Kumaresan S, Xiao L, Mernaugh RL, Itani HA, Loperena R, Chen W, Dikalov S, Titze JM, Knollmann BC, Harrison DG, Kirabo A. Dendritic Cell Amiloride-Sensitive Channels Mediate Sodium-Induced Inflammation and Hypertension. *Cell Rep*. 2017;21(4):1009-1020. doi:10.1016/j.celrep.2017.10.002

33. Takahashi H, Nakagawa S, Wu Y, Kawabata Y, Numabe A, Yanagi Y, Tamaki Y, Uehara Y, Araie M. A high-salt diet enhances leukocyte adhesion in association with kidney injury in young Dahl salt-sensitive rats. *Hypertens Res*. 2017;40(11):912-920. doi:10.1038/hr.2017.31

34. Hernandez AL, Kitz A, Wu C, Lowther DE, Rodriguez DM, Vudattu N, Deng S, Herold KC, Kuchroo VK, Kleinewietfeld M, Hafler DA. Sodium chloride inhibits the suppressive function of FOXP3+ regulatory T cells. *J Clin Invest*. 2015;125(11):4212-4222. doi:10.1172/JCI81151

35. Mattson DL. Infiltrating immune cells in the kidney in salt-sensitive hypertension and renal injury. *Am J Physiol Renal Physiol*. 2014;307(5):F499-508. doi:10.1152/ajprenal.00258.2014

36. Bernhardt A, Krause A, Reichardt C, Steffen H, Isermann B, Völker U, Hammer E, Geffers R, Philipsen L, Dhjamandi K, Ahmad S, Brandt S, Lindquist JA, Mertens PR. Excessive sodium chloride ingestion promotes inflammation and kidney fibrosis in aging mice. *Am J Physiol Cell Physiol*. 2023;325(2):C456-C470. doi:10.1152/ajpcell.00230.2023

37. Ruggeri Barbaro N, Van Beusecum J, Xiao L, do Carmo L, Pitzer A, Loperena R, Foss JD, Elijovich F, Laffer CL, Montaniel KR, Galindo CL, Chen W, Ao M, Mernaugh RL, Alsouqi A, Ikizler TA, Fogo AB, Moreno H, Zhao S, Davies SS, Harrison DG, Kirabo A. Sodium activates human monocytes via the NADPH oxidase and isolevuglandin formation. *Cardiovasc Res*. 2021;117(5):1358-1371. doi:10.1093/cvr/cvaa207

38. Tomino Y, Ohmuro H, Kuramoto T, Shirato I, Eguchi K, Sakai H, Okumura K, Koide H. Expression of intercellular adhesion molecule-1 and infiltration of lymphocytes in glomeruli of patients with IgA nephropathy. *Nephron*. 1994;67(3):302-307. doi:10.1159/000187984

39. Müller GA, Markovic-Lipkovski J, Müller CA. Intercellular adhesion molecule-1 expression in human kidneys with glomerulonephritis. *Clin Nephrol*. 1991;36(4):203-208.

40. Arrizabalaga P, Solé M, Abellana R, de las Cuevas X, Soler J, Pascual J, Ascaso C. Tubular and interstitial expression of ICAM-1 as a marker of renal injury in IgA nephropathy. *Am J Nephrol*. 2003;23(3):121-128. doi:10.1159/000068920

41. Li S, Mariappan N, Megyesi J, Shank B, Kannan K, Theus S, Price PM, Duffield JS, Portilla D. Proximal tubule PPARα attenuates renal fibrosis and inflammation caused by unilateral ureteral obstruction. *Am J Physiol Renal Physiol*. 2013;305(5):F618-627. doi:10.1152/ajprenal.00309.2013

42. Park CW, Kim HW, Ko SH, Chung HW, Lim SW, Yang CW, Chang YS, Sugawara A, Guan Y, Breyer MD. Accelerated diabetic nephropathy in mice lacking the peroxisome proliferator-activated receptor alpha. *Diabetes*. 2006;55(4):885-893. doi:10.2337/diabetes.55.04.06.db05-1329

43. Ozata DM, Gainetdinov I, Zoch A, O'Carroll D, Zamore PD. PIWI-interacting RNAs: small RNAs with big functions. *Nat Rev Genet*. 2019;20(2):89-108. doi:10.1038/s41576-018-0073-3

44. Wang X, Ramat A, Simonelig M, Liu MF. Emerging roles and functional mechanisms of PIWI-interacting RNAs. *Nat Rev Mol Cell Biol*. 2023;24(2):123-141. doi:10.1038/s41580-022-00528-0

45. Piuco R, Galante PAF. piRNAdb: A piwi-interacting RNA database. Published online September 24, 2021:2021.09.21.461238. doi:10.1101/2021.09.21.461238

46. International Consortium for Blood Pressure Genome-Wide Association Studies, Ehret GB, Munroe PB, Rice KM, Bochud M, Johnson AD, Chasman DI, Smith AV, Tobin MD, Verwoert GC, Hwang SJ, Pihur V, Vollenweider P, O'Reilly PF, Amin N, Bragg-Gresham JL, Teumer A, Glazer NL, Launer L, Zhao JH, Aulchenko Y,

Heath S, Sõber S, Parsa A, Luan J, Arora P, Dehghan A, Zhang F, Lucas G, Hicks AA, Jackson AU, Peden JF, Tanaka T, Wild SH, Rudan I, Igl W, Milaneschi Y, Parker AN, Fava C, Chambers JC, Fox ER, Kumari M, Go MJ, van der Harst P, Kao WHL, Sjögren M, Vinay DG, Alexander M, Tabara Y, Shaw-Hawkins S, Whincup PH, Liu Y, Shi G, Kuusisto J, Tayo B, Seielstad M, Sim X, Nguyen KDH, Lehtimäki T, Matullo G, Wu Y, Gaunt TR, Onland-Moret NC, Cooper MN, Platou CGP, Org E, Hardy R, Dahgam S, Palmen J, Vitart V, Braund PS, Kuznetsova T, Uiterwaal CSPM, Adeyemo A, Palmas W, Campbell H, Ludwig B, Tomaszewski M, Tzoulaki I, Palmer ND, CARDIoGRAM consortium, CKDGen Consortium, KidneyGen Consortium, EchoGen consortium, CHARGE-HF consortium, Aspelund T, Garcia M, Chang YPC, O'Connell JR, Steinle NI, Grobbee DE, Arking DE, Kardia SL, Morrison AC, Hernandez D, Najjar S, McArdle WL, Hadley D, et al. Genetic variants in novel pathways influence blood pressure and cardiovascular disease risk. *Nature*. 2011;478(7367):103-109. doi:10.1038/nature10405

47. Tomaszewski M, Eales J, Denniff M, Myers S, Chew GS, Nelson CP, Christofidou P, Desai A, Büsst C, Wojnar L, Musialik K, Jozwiak J, Debiec R, Dominiczak AF, Navis G, van Gilst WH, van der Harst P, Samani NJ, Harrap S, Bogdanski P, Zukowska-Szczechowska E, Charchar FJ. Renal Mechanisms of Association between Fibroblast Growth Factor 1 and Blood Pressure. *J Am Soc Nephrol*. 2015;26(12):3151-3160. doi:10.1681/ASN.2014121211

48. Allison SJ. Indian Hedgehog links kidney injury to fibrosis. *Nat Rev Nephrol*. 2023;19(8):478. doi:10.1038/s41581-023-00735-8